Hindawi Publishing Corporation
Advances in Condensed Matter Physics
Volume 2008, Article ID 817829, 23 pages
doi:10.1155/2008/817829

Review Article

Viscosity and Glass Transition in Amorphous Oxides

Michael I. Ojovan

Department of Engineering Materials, The University of Sheffield, Sir Robert Hadfield Building, Mappin Street, Sheffield S1 3JD, UK

Correspondence should be addressed to Michael I. Ojovan, m.ojovan@sheffield.ac.uk

Received 12 June 2008; Revised 20 October 2008; Accepted 7 December 2008

Recommended by Mark Bowick

An overview is given of amorphous oxide materials viscosity and glass-liquid transition phenomena. The viscosity is a continuous function of temperature, whereas the glass-liquid transition is accompanied by explicit discontinuities in the derivative parameters such as the specific heat or thermal expansion coefficient. A compendium of viscosity models is given including recent data on viscous flow model based on network defects in which thermodynamic parameters of configurons—elementary excitations resulting from broken bonds—are found from viscosity-temperature relationships. Glass-liquid transition phenomena are described including the configuron model of glass transition which shows a reduction of Hausdorff dimension of bonds at glass-liquid transition.

1. Introduction

Solids can be either amorphous or crystalline in structure. In the solid-state, elementary particles (atoms, molecules), which form the substance, are in fixed positions arranged in a repeating pattern in crystalline solids or in a disordered pattern in amorphous solids. The structures of crystalline solids are formed of repeating regular units, for example, unit cells. Each unit cell of a crystal is defined in terms of lattice points, for example, the points in space about which the particles are free to vibrate. The structure of amorphous materials cannot be described in terms of repeating unit cells; because of nonperiodicity, the unit cell of an amorphous material would comprise all atoms. Both solid-state physics and chemistry focus almost entirely on crystalline form of matter [1–3], whereas the physics and chemistry of amorphous state in many aspects remain poorly understood. Although numerous experiments and theoretical works have been performed, many of the amorphous-state features remain unexplained and others are controversial. One of such controversial problems is the nature of glass-liquid transition. The difficulty in treating the glass transition is caused by almost undetectable changes in the structure despite the qualitative changes in characteristics and extremely large change in the time scale [4]. The translation-rotation symmetry of particles is unchanged at the liquid-glass transition, which retains the topological disorder of fluids. Like a liquid, a glass has a topologically disordered distribution of atoms and molecules but elastic properties of an isotropic solid. The symmetry similarity of both liquid and glassy phases leaves unexplained qualitative differences in their behaviour. We demonstrate below that there is a qualitative difference in the symmetries of liquid and glasses when the system of joining bonds is examined rather than the distribution of material elementary particles.

According to the nature of the bonds which hold particles together, condensed materials can be classified as metallic, ionic, molecular, or covalent network solids or fluids. For example, the principal types of binding are caused by collective electrons in metals, electrostatic forces between positive and negative ions in ionic materials, overlapping electron distributions in covalent structures, and van der Waals forces in molecular substances [2]. One of the useful approaches is to consider the bond system instead of considering the set of atoms or molecules that form the matter. For each state of matter, we can define the set of bonds, for example, introduce the bond lattice model which is the congruent structure of its chemical bonds. The congruent bond lattice is a regular structure for crystalline materials and disordered for amorphous materials. A configuron is defined as an elementary configurational excitation in an amorphous material which involves breaking of a chemical

bond and associated strain-releasing local adjustment of centres of atomic vibration. The higher the temperature of an amorphous material is, the higher the configuron concentration is. Configurons weaken the bond system, so that the higher the content of configurons is, the lower the viscosity of an amorphous material is. At very high concentrations, configurons form percolation clusters. This means that the material loses its rigidity as it becomes penetrated by a macroscopic (infinite-size) clusters made of broken bonds. The formation of percolation clusters made of configurons gives an explanation of glass transition in terms of percolation-type phase transitions [5]. Moreover, although no symmetry changes can be revealed in the atomic distribution, there is a stepwise variation of Hausdorff dimension of bonds at the glass transition, namely, there is a reduction of Hausdorff dimension of bonds from the 3 in the glassy state to the fractal $d_f = 2.55 \pm 0.05$ in the liquid state [5, 6].

We give an overview of viscosity and glass-transition phenomena in amorphous oxides in this paper. Viscosity-temperature relationships and viscosity models are considered including recent data on viscous flow model based on network defects in which thermodynamic parameters of configurons—elementary excitations resulting from broken bonds in amorphous oxides—are found from viscosity-temperature relationships. Glass-liquid transition phenomena are described along with the configuron model of glass transition in which the Hausdorff dimension of material bond system changes at glass transition.

2. Amorphous Oxide Materials

Oxides are the most abundant inorganic substances on the Earth and at the same time among the most important materials for practical applications. Oxide materials are of excellent environmental stability [7, 8]. They are used in many applications from home cookware to industrial thermal insulations and refractories as well as nuclear waste immobilisation [9]. Oxide materials exist in a wide variety of chemical compositions and crystal structures. However, oxide materials are most frequently found in disordered, for example, amorphous state. There is an enormous diversity of amorphous materials, including covalently-bonded oxide glasses such as vitreous silica, the structure of which is modelled by a continuous random network of bonds (network-forming materials); metallic glasses bonded by isotropic pair potentials, whose structure is thought of as a dense random packing of spheres; amorphous polymers, whose structure is assumed to be an arrangement of interpenetrating random-walk-like coils strongly entangled with each other. Silicate glasses are representative examples of widely used oxide amorphous materials with everyday importance.

Although disordered, the oxide materials in the most frequently used glassy state exhibit similar mechanical properties to crystalline materials. The International Commission on Glass defines glass as a uniform amorphous solid material, usually produced when the viscous molten material cools very rapidly to below its glass transition temperature, without sufficient time for a regular crystal lattice to form [10]. The IUPAC Compendium on Chemical Terminology defines glass transition as a second-order transition in which a supercooled melt yields, on cooling, a glassy structure [11]. It states that below the glass-transition temperature, the physical properties of glasses vary in a manner similar to those of the crystalline phase. Moreover, it is deemed that the bonding structure of glasses although disordered has the same symmetry signature (Hausdorff-Besikovitch dimensionality) as for crystalline materials [6, 12].

Glass is one of the most ancient of all materials known and used by mankind. The natural glass, obsidian, was first used by man thousands of years ago to form knives, arrow tips, and jewellery. Manmade glass objects from Mesopotamia have been dated as early as 4500 BC and from Egypt from 3000 BC. The high chemical resistance of glass allows it to remain stable in corrosive environments for many thousands and even millions of years. Several glasses are found in nature such as obsidians (volcanic glasses), fulgarites (formed by lightning strikes), tektites found on land in Australasia and associated microtektites from the bottom of the Indian Ocean, moldavites from central Europe, and Libyan Desert glass from western Egypt. Some of these glasses have been in the natural environment for about 300 million years with low alteration rates of less than a millimetre per million years. For example, the natural glass obsidian is formed when lava erupts from volcanoes and cools rapidly without sufficient time for crystal growth. The composition of a typical California obsidian is (wt%) $75SiO_2$ $13.5Al_2O$ $1.6FeO/Fe_2O_3$ $1.4CaO$ $4.3Na_2O$ $4.5K_2O$ $0.7MnO$. Obsidian glass edges can be extremely sharp reaching almost molecular thinness and was known for its ancient use as knives and projectile tips. Tektites are other natural glasses, typically up to a few centimetres in size, which have most probably been formed by the impact of large meteorites on the Earth surface which melted the Earth surface material resulting on cooling in glass. The age of tektites found in Czech Republic, moldavites of typical composition $(75–80)SiO_2$ $(9–12)Al_2O$ $(1–3)FeO/Fe_2O_3$ $(2-3)CaO$ $0.3Na_2O$ $3.5K_2O$, is assessed to be approximately 15 million years [7].

Glasses are most frequently produced by a melt cooling below its glass-transition temperature sufficiently fast to avoid formation of crystalline phases. Glass-forming materials such as dioxides do not require very fast cooling, whereas quickly crystallising materials such as metals require a very fast cooling (quenching), for example, the early metallic glasses had to be cooled extremely rapidly $\sim 10^6$ K/s to avoid crystallisation [13, 14]. Glasses can be formed by several methods such as

(i) melt quenching [7];

(ii) physical vapour deposition [15];

(iii) solid-state reactions (thermochemical [16] and mechanochemical [17] methods);

(iv) liquid-state reactions (sol-gel method [18, 19]);

(v) irradiation of crystalline solids (radiation amorphisation [20, 21]);

Table 1: Commercial oxide glass compositions.

Glass family (application)	Oxide, mass %									
	SiO_2	Na_2O	CaO	Al_2O_3	MgO	B_2O_3	BaO	PbO	K_2O	ZnO
Vitreous silica (Furnace tubes, Si melting crucibles)	100									
Soda-lime silicate:										
Window	72.0	14.2	10.0	0.6	2.5		trace		0.6	
Container	74.0	15.3	5.4	1.0	3.7				0.6	
Bulb and tube	73.3	16.0	5.2	1.3	3.5					
Tableware	74.0	18.0	7.5	0.5						
Sodium borosilicate:										
Chemical glassware	81.0	4.5		2.0		12.0				
Waste immobilisation	43–53	6–24	0–14	3–19	0–5.3	8–17	misc.	misc.	misc.	misc.
Lead-alkali silicate:										
Lead "crystal"	59.0	2.0		0.4				25.0	12.0	1.5
Television funnel	54.0	6.0	3.0	2.0	2.0			23.0	8.0	
Aluminosilicate:										
Halogen lamp	57.0	0.01	10.0	16.0	7.0	4.0	6.0		trace	
Fibreglass "E"	52.9		17.4	14.5	4.4	9.2			1.0	
Optical (crown)	68.9	8.8				10.1	2.8		8.4	1.0

(vi) under action of high pressures (pressure amorphisation [22, 23]).

Glass formation from melts is a matter of bypassing crystallisation, and formation of glass is easier in more complex systems. Oxide glasses containing a variety of cations are easier to be obtained in a glassy state as their complexity necessitates longer times for diffusion-controlled redistribution of diverse constituents before crystallisation can begin. The vast bulk of glasses used in commerce are oxide glasses. It is assessed that better than 95% of the commercial tonnage is oxide glasses, of which ~95% is silica-based glasses [5]. Table 1 gives the composition of important oxide glasses [7, 24, 25].

3. Melting of Amorphous Solids

Crystalline materials melt at well-defined melting temperatures T_m whereas amorphous materials transform from glassy, for example, solid form to liquid-state at glass transition temperatures T_g which in this sense play the role of melting temperatures for non-crystalline solids. Although fundamentally important, the nature of the glass transition is not well understood [25–30]. A glass is most commonly formed by cooling a viscous liquid fast enough to avoid crystallisation. Compared with T_m, the actual values of T_g depend on thermal history, for example, cooling rate which makes the understanding of glass transition phenomena intriguing. The liquid-glass transition is accompanied by significant changes in physical properties, for example, glasses are brittle, thus changes should occur at the molecular level although the material is topologically disordered both in liquid and glassy states. Rearrangements that occur in an amorphous material at the glass transition temperature lead to characteristic discontinuities of derivative thermodynamic parameters such as the coefficient of thermal expansion [31] or the specific heat (Figure 1).

These discontinuities allow detecting the T_g [31] or, accounting for cooling rate dependences, the glass transition interval where a supercooled liquid transforms to a glass (Figure 2).

Vitrification manifests itself as a second-order phase transition, however its description in terms of the Landau theory is difficult as there is no clarity about the order parameter describing this transition [33, 34]. Although similar to a second-order phase transformation, the glass-liquid transition is a kinetically controlled phenomenon which exhibits a range of T_g depending on the cooling rate with maximal T_g at highest rates of cooling [31]. In practice, the liquid-glass transition has features both in common with second-order thermodynamic phase transitions and of kinetic origin. Glass-forming material commonly exhibits two types of relaxation process: fast β relaxation (Johari-Goldstein) and slow α relaxation [29, 30]. The attention of the majority of researchers in the last decades has been focused on relaxation aspects of the liquid-glass transition rather than the structure [29]. Emphasis in these works is placed on glass nonergodicity and it is considered that glass is a material characterised by large Deborah numbers [35] for which the relaxation time is much longer than the observation time taken typically as 10^2 seconds. The systems are commonly assumed to be ergodic at temperatures $T > T_g$, whereas the systems are completely frozen with respect to primary relaxation at $T < T_g$ [29, 36]. Figure 3(a) shows three regions of amorphous materials behaviour based on the temperature variations of extensive thermodynamic

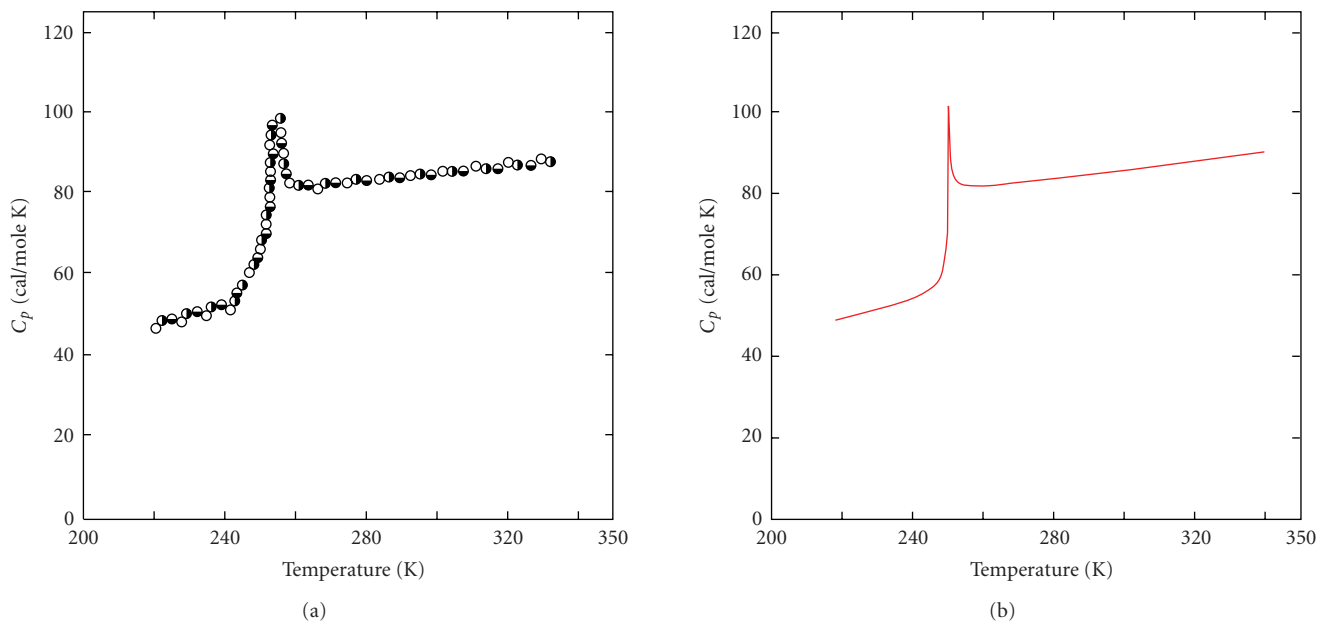

Figure 1: Specific heat of amorphous *o*-terphenil. (a) Experimental and (b) calculated [12].

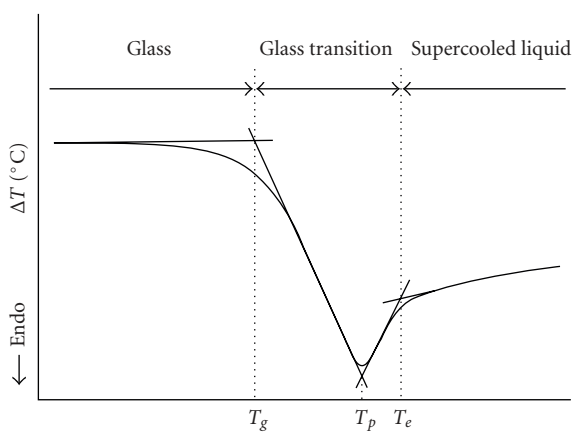

Figure 2: Determination of glass transition temperature T_g based on differential temperature analysis (DTA), below the T_g the material is glassy whereas above the T_e the material is liquid (after [32]).

parameters, for example, enthalpy (H) and specific volume (V) [29]: (a) ergodic, (b) transition, and (c) nonergodic. Goldstein found that diffusion in liquids occurs by different mechanisms at high and low temperatures. Jump potential energy barriers are large at low temperatures, while at high temperatures molecules move almost freely since thermal energies overcome the barrier heights [37]. The correlation between the energy landscape and the fragility of liquids was emphasised by Angell [38]. Recent works [5, 6, 12] have revealed that in addition to changes in relaxation behaviour, significant changes occur within the system of bonds at glass-liquid transition (Figure 3(b)).

As on cooling, the viscosities of glass-forming liquids continuously increase and achieve very high values, the liquid-glass transition is often regarded as a transition for practical purposes rather than a thermodynamic phase transition [2, 39]. By general agreement, it is considered that a liquid on being cooled becomes practically a glass when the viscosity equals 10^{12} Pa·s (10^{13} poise) or where the relaxation time is 10^2 seconds [2, 39]. There is no phase transformation at this practical purpose (relaxation) glass-transition temperature [2] which is found from the viscosity-temperature relationship:

$$\eta(T_{g,\mathrm{relax}}) = 10^{12}(\mathrm{Pa{\cdot}s}). \tag{1}$$

Despite the fact that a glass like a liquid has a topologically disordered structure, at the same time, it has elastic properties of an isotropic solid. Changes should thus occur at the molecular level although the material is topologically disordered both in liquid and glassy states. The difficulty is to specify how the structure of a glassy material differs from that one of a liquid. The translation-rotation symmetry in the distribution of atoms and molecules is broken at crystallisation but remains unchanged at the liquid-glass transition, which retains the topological disorder of fluids.

What kind of symmetry is changed at glass-liquid transition? Amorphous materials have no elementary cell characterised by a certain symmetry, which can reproduce the distribution of atoms by its infinite repetition. Instead the symmetry of a topologically disordered system is characterised by the Hausdorff-Besikovitch dimensionality of the system bonds. Formally, the Hausdorff dimension of a subset A of a metric space X is the infimum (e.g., the greatest element, not necessarily in the subset, that is less than or equal to all other elements of the subset) of $d \geq 0$ such that the d-dimensional Hausdorff measure of A is 0 (which need not be integer) [40]. In practice, the Hausdorff dimension is defined using the standard procedure of covering the subset

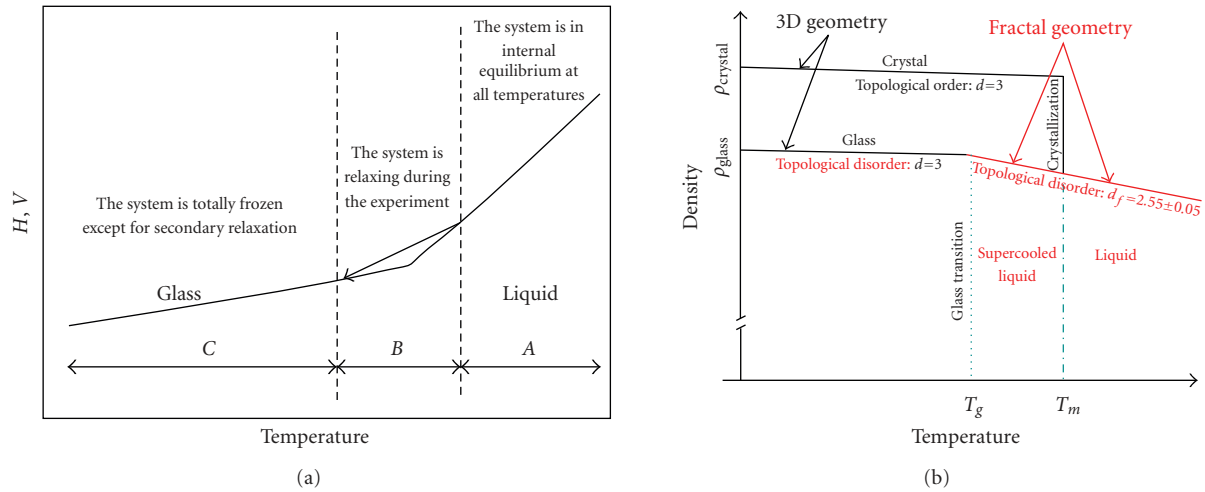

Figure 3: (a) Regions of relaxation behaviour of amorphous materials (after [29]); (b) density and geometry of bonds on increase of temperature (after [6]).

considered (congruent bond structure in our case) with a number $N(\lambda)$ of spheres of radius λ (or cubes with size λ). In condensed matter, the smallest size possible for λ is the bond size. The smaller the λ is, the larger the $N(\lambda)$ is, and the fractal dimension is found as the limiting case from

$$d_f = -\lim_{\lambda \to 0} \frac{\log N(\lambda)}{\log \lambda}. \quad (2)$$

Roughly, if $N(\lambda)$ grows proportionally to $1/\lambda^d$ as λ tends to zero, then we say that the subset has the Hausdorff dimension d [41]. Using such a procedure, we could find that 3-dimensional bond structures, which have joining bonds intact, are characterised by the Hausdorff dimension $d = 3$. This conforms to the known result that the Euclidian space R^n has the Hausdorff dimension, $d = n$. Moreover, whether the distribution of bonds is ordered or disordered is unimportant, in both cases the 3-dimensional bond structures have the same Hausdorff dimension, $d = 3$. Thus, in both cases, for example, in both glasses and crystals we have the same Hausdorff dimension of the bond system.

Two types of topological disorder characterised by different symmetries can be revealed in an amorphous material based on the analysis of broken bond concentrations [5, 6, 12]: (i) 3-dimensional, 3D (Euclidean, $d = 3$), which occurs at low temperatures when the configurons are uniformly distributed within the bond structure with no percolation clusters of configurons formed and the geometrical structures of bonds can be characterised as a 3D and (ii) $d_f = 2.55 \pm 0.05$-dimensional (fractal), which occurs at high temperatures at least near the glass transition temperature when percolation clusters made of broken bonds are formed and the geometries of the dynamic structures formed can be characterised as fractal objects with preferential pathways for configurons. Hence, the bonding structure of glasses has the same Hausdorff-Besikovitch dimensionality (symmetry signature) as for crystalline materials (Figure 3(b)) whereas the liquid near the glass transition is a dynamic uniform fractal. We will first consider herein the viscosity of amorphous materials and then analyse models of glass-liquid transition. Although we do not directly link the melting of amorphous materials (e.g., glass-liquid transition) with their viscosity (see (1)), we will use the viscosity-temperature relationships to identify the thermodynamic parameters of configurons.

Table 2: Viscosity of some amorphous materials.

Material	Viscosity, Pa·s
Water at 25°C	$0.894\ 10^{-3}$
Mercury at 25°C	$1.526\ 10^{-3}$
Olive oil at 25°C	$8.1\ 10^{-2}$
Glycerol at 25°C	0.934
Glass batch at melting point	10
Pitch at 25°C	$2.3\ 10^{8}$
Glass at strain point	$3\ 10^{13}$

4. Viscosity-Temperature Relationships

The viscosities of fluids are among their most important properties. Viscosity quantifies the resistance of fluids to flow and indicates their ability to dissipate momentum. The momentum balance of the Newtonian fluids is described at the macroscopic level by the Navier-Stokes equations. At the microscopic level, viscosity arises because of a transfer of momentum between fluid layers moving at different velocities as explained in the Maxwell kinetic theory. In oxide melts and glasses, viscosities determine melting conditions, working and annealing temperatures, rate of refining, maximum use temperature, and crystallisation rate. In geology, the behaviour of magma and hence volcanic eruptions and lava flow rates depend directly on the viscosities of molten silicates [42, 43]. Table 2 gives viscosities of several amorphous materials.

It is commonly assumed that shear viscosity is a thermally activated process. Since the pioneering work of Frenkel

[44] fluid viscosity, $\eta(T)$, has been expressed in terms of an activation energy Q by

$$\eta(T) = A \exp\left(\frac{Q}{RT}\right), \tag{3}$$

where T is temperature in K, R is the molar gas constant, and A is a constant. For amorphous materials, two different regimes of flow have been identified with melts at high temperature having lower activation energy for flow than materials at lower temperatures. Within the low temperature or high temperature regimes, an Arrhenius dependence of viscosity is observed and an appropriate activation energy, Q_H or Q_L, respectively, can be defined. Asymptotically, both at low and high temperatures the activation energy of viscosity is independent of temperature. This pattern has been observed with a range of melts including silicates, fused salts, oxides, and organic liquids [42, 43]. Between the high temperature and the low temperature regimes, the activation energy for flow changes and the viscosity cannot be described using the Arrhenius-type behaviour, for example, the activation energy of viscosity varies with temperature.

Viscosity directly governs the relaxation processes in amorphous materials. The Maxwell relaxation time gives the characteristic relaxation time to attain stabilised parameters of a material:

$$\tau_M = \frac{\eta}{G}, \tag{4}$$

where G is the shear modulus. The higher the viscosity is, the longer the relaxation times are. Near the glass-transition temperature, the elasticity modulus of a glass $G \sim 10^{10}$ Pa [45], hence at $\eta = 10^{12}$ Pa·s, where the practical purpose (relaxation) glass transition occurs (see (1)), the Maxwell relaxation time $\tau_M \sim 10^2$ seconds. Accounting that for fused silica the activation energy of viscosity at low temperatures $Q_H = 759$ kJ/mol and the shear modulus of fused silica is 31 GPa at 25°C [46, 47], one can see that the relaxation time at STP becomes as long as $\tau_M \sim 10^{98}$ years which incommensurably exceeds the lifetime of Universe (approx. 1.5×10^{10} years). This shows again that the glass should be considered a true solid material [48].

The viscosity of amorphous materials depends on chemical composition, for example, in silicate systems viscosity attains the highest values for vitreous silica (Figure 4).

The more or less randomness, the openness, and the varying degree of connectivity allow the glass structure to accommodate large variations in composition, for example, glass acts like a solution. Moreover, it was found that melts and glasses produced from them can be often considered as solutions consisting of salt-like products of interactions between the oxide components [50]. These associates are similar to the crystalline compounds which exist in the phase diagram of the initial oxide system. Calculations in this model are based on solving the set of equations for the law of mass action for the reactions possible in the system of oxides and the equations of mass balance of the components. This approach describes well such properties as viscosity,

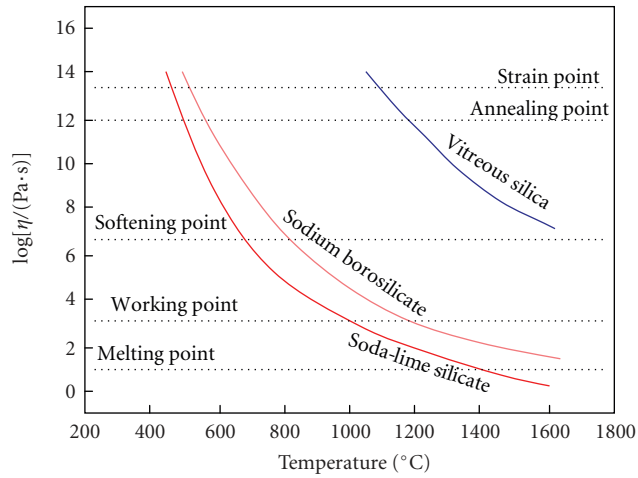

Figure 4: Viscosity of amorphous silicates and important technological points in glass manufacture industry (after [49]).

thermal expansion, isothermal compressibility, and optical parameters [50].

For oxide glasses, a small change in glass composition typically causes a smooth change in glass properties. The unit addition or substitution of a component can be deemed as a contribution characteristic of that component to the overall property. This notion gives rise to the additive relationships with many properties such as densities, refractive indexes obeying additive relationships [7]. An additive property P obeys a linear relation of the type

$$P = \sum_{i=1}^{n} p_i C_i, \quad \text{where} \sum_{i=1}^{n} C_i = 100\%, \tag{5}$$

where p_i are additivity factors for a given component $i = 1, 2, 3, \ldots, n$, and C_i are the mass% or the mol% of that component in the glass. In oxide glasses, the density follows additivity primarily because the volume of an oxide glass is mostly determined by the volume occupied by the oxygen anions, the volume of cations being much smaller [7]. Additivity relations work over a narrow range of compositions and additivity coefficients of a given oxide may change from system to system. Nonlinearities appear when various constituents interact with each other. Glass properties can be calculated through statistical analysis of glass databases such as SciGlass [7, 51]. Linear regression can be applied using common polynomial functions up to the 2nd or 3rd degrees. For viscosities of amorphous oxide materials (melts and glasses), the statistical analysis of viscosity is based on finding temperatures (isokoms) of constant viscosity $\log[\eta(T_i)] = \text{const}_i$, typically when viscosity is 1.5, 6.6, and 12 (point of practical purpose glass transition) [51–53]. A detailed overview on statistical analysis of viscosities and individual oxide coefficients C_i in isokom temperatures of oxide materials is given in [53]. Addition of oxides to certain base compositions changes the viscosity and the impact from different oxides is different [5, 51–54]. Figure 5 shows the effect of component addition

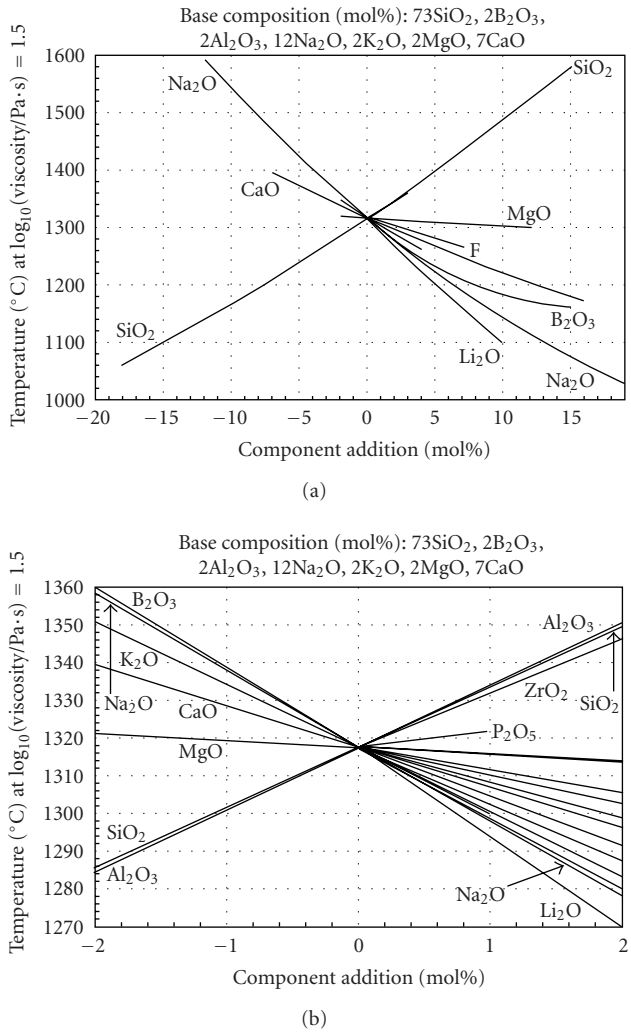

Figure 5: Effect of component addition on isokom $\log[\eta(T)/\text{Pa}\cdot\text{s}] = 1.5$ [53]. Courtesy Alexander Fluegel.

to the base composition in mol% $73SiO_2$ $2B_2O_3$ $2Al_2O_3$ $12Na_2O$ $2K_2O$ 2MgO 7CaO on the temperature where the viscosity $\log(\eta(T)) = 1.5$ (isokom) [53].

5. Fragility Concept

As noted above, the term glass transition temperature is often used to refer to the temperature at which the viscosity attains a value of 10^{12} Pa·s. This definition of T_g was used by Angell to plot the logarithms of viscosity as a function of (T_g/T) [55, 56]. In such a plot, strong melts, *that is*, melts that exhibit only small changes in the activation energy for flow with temperature, such as silica or germania, have a nearly linear dependence on the inverse of the reduced temperature whereas fragile melts deviate strongly from a linear dependence as the activation energies of fragile liquids significantly change with temperature. However, this change is characteristic only for intermediate temperatures and the viscosity has asymptotically Arrhenius-type behaviour both at high and low temperatures. Within the low temperature, the activation energy of viscosity is high Q_H whereas at high temperatures the activation energy is low Q_L. As asymptotically, both at low and high temperatures the activation energies of viscosity are independent of temperature changes that occur in the activation energy can be unambiguously characterised by the Doremus fragility ratio [42, 43]:

$$R_D = \frac{Q_H}{Q_L}. \tag{6}$$

The Doremus fragility ratio ranges from 1.45 for silica to 4.52 for anorthite melts (Table 3).

The higher the value of R_D is, the more fragile the melt is. The fragility of amorphous materials numerically characterised by the Doremus fragility ratio classifies amorphous materials as strong if they have $R_D < 2$, and fragile materials if they have $R_D \geq 2$. The implication of strong-fragile classification was that strong fluids are strongly and fragile are weakly bonded [56]. As pointed out by Doremus [42, 43], these widely and convenient terms are misleading, for example, binary silicate glasses are strong although have many nonbridging oxygens. Some network melts such as anorthite and diopside have very high activation energies being quite strongly bounded but are very fragile. Nevertheless, the fragility concept enables classification of melts based on their viscosity behaviour. Those melts which significantly change the activation energy of viscosity are fragile and those which have small changes of activation energy of viscosity are strong.

6. Viscosity Models

Many different equations to model the viscosity of liquids have been proposed. The first one is the Frenkel-Andrade model which assumes that viscosity is a thermally activated process described by a simple exponential equation (3) with constant activation energy of viscosity [44]. As this simple model fails to describe the behaviour of viscosity at intermediate temperatures between strain and melting points (see Figure 4), many other models were developed some of which become popular and are being extensively used. Although it is well known [57, 58] that the best description of viscosity is given by the two-exponential equation derived by Douglas [59], the most popular viscosity equation is that of Vogel, Tamman and Fulcher (VTF). It gives an excellent description of viscosity behaviour, namely, at intermediate temperatures which are very important for industry. It is also most useful in describing the behaviour of amorphous materials in the transition range (range B on Figure 3(a)), where solidification of amorphous materials occurs. Adam-Gibbs (AG) and Avramov-Milchev (AM) models are also often used to describe the viscosity in the intermediate range of temperatures. Out of the intermediate range, none of these models correctly describe the behaviour of viscosity and in the limits of low and high temperatures the best description of viscosity provides the Frenkel-Andrade model with high and low activation energies. Moreover, there is a tendency to a nonactivated regime of viscosity of melts at very high-temperatures [47]. Figure 6 summarises the temperature

Table 3: Asymptotic Arrhenian activation energies for viscosity and the corresponding Doremus fragility ratios [47].

Amorphous material	Q_L, kJ/mol	Q_H, kJ/mol	R_D
Silica (SiO_2)	522	759	1.45
Germania (GeO_2)	272	401	1.47
$66.7SiO_2$ 33.3PbO	274	471	1.72
$80SiO_2$ $20Na_2O$	207	362	1.75
$65SiO_2$ 35PbO	257	488	1.9
$59.9SiO_2$ 40.1PbO	258	494	1.91
$75SiO_2$ $25Na_2O$	203	436	2.15
$75.9SiO_2$ 24.1PbO	234	506	2.16
SLS: $70SiO_2$ 21CaO $9Na_2O$	293	634	2.16
Salol ($HOC_6H_4COOC_6H_5$)	118	263	2.23
$70SiO_2$ $30Na_2O$	205	463	2.26
$65SiO_2$ $35Na_2O$	186	486	2.61
α-phenyl-o-cresol (2- Hydroxydiphenylmethane)	103	275	2.67
$52SiO_2$ $30Li_2O$ $18B_2O_3$	194	614	3.16
B_2O_3	113	371	3.28
Diopside ($CaMgSi_2O_6$)	240	1084	4.51
Anorthite ($CaAl_2Si_2O_8$)	251	1135	4.52

behaviour of viscosity within various temperature intervals and indicates the character of activation energy of viscosity with best equations to be used including the equation of viscosity valid at all temperatures (see below (12)).

6.1. VTF Model

The VTF equation of viscosity is an empirical expression which describes viscosity data at intermediate temperatures (see Figure 6) over many orders of magnitude with a high accuracy:

$$\ln\left[\eta(T)\right] = A_{\mathrm{VTF}} + \frac{B_{\mathrm{VTF}}}{R(T - T_V)}, \tag{7}$$

where A_{VTF}, B_{VTF}, and T_V (Vogel temperature) are constants determined by fitting (7) to experimental data. Although perfectly working at intermediate temperatures at high and low temperatures, (7) does not describe the experimental temperature dependence of viscosity.

The VTF equation can be derived from the free volume model which relates the viscosity of the melt to free (or excess) volume per molecule V_f. The excess volume is considered to be the specific volume of the liquid minus the volume of its molecules. This molecular volume is usually derived from a hard sphere model of the atoms in the molecules. Molecular transport is considered to occur when voids having a volume greater than a critical value form by redistribution of the free volume [60]. The flow unit or molecule is imagined to be in a structural cage at a potential minimum. As the temperature increases, there is an increasing amount of free volume that can be redistributed among the cages, leading to increased transport and this

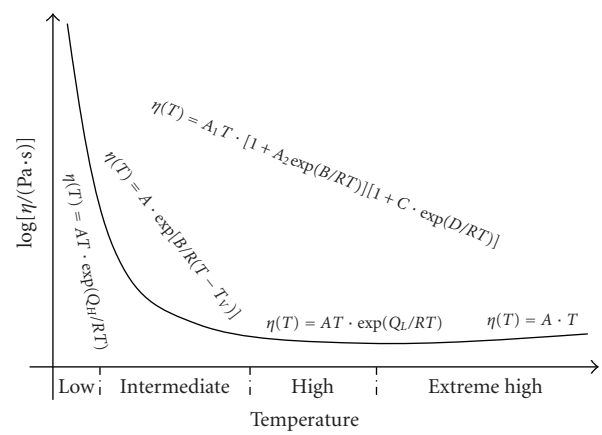

Figure 6: Temperature behaviour of viscosity of amorphous materials as described by the universal equation (12). The activation energy of viscous flow is constant and high at low temperatures, it is variable at intermediate temperatures, and it is constant and low at high temperatures. At extreme high temperatures, the flow becomes nonactivated.

leads to an exponential relationship between viscosity and free volume [60]:

$$\eta = \eta_0 \exp\left(\frac{BV_0}{V_f}\right), \tag{8}$$

where V_0 is the volume of a molecule, η_0 and B are constants. In terms of the specific volume V per molecule, it can be shown that $V_f = V - V_0 = V_0(T - T_0)/T_0$, for some constant and low temperatures T_0. Clearly, (8) is the same as (7) when $A_{\mathrm{VTF}} = \ln\eta_0$, $B_{\mathrm{VTF}} = BT_0$ and $T_V = T_0$. The generic problem with the free volume theory is that the specific volume of a liquid as a function of temperature shows a

discontinuity in slope at the glass transition temperature (see Figure 3(b)), whereas the viscosities of liquids show no discontinuities at the glass transition temperature [43].

6.2. Adam and Gibbs Model

The Adam and Gibbs (AG) equation is obtained assuming that above the glass transition temperature molecules in a liquid can explore many different configurational states over time, and that as the temperature is raised higher energy configurational states can be explored. In contrast, below the glass transition temperature it is assumed that the molecules in the glass are trapped in a single configurational state. The resulting AG equation for viscosity is similar to the VTF equation [61]:

$$\ln[\eta(T)] = A_{\mathrm{AG}} + \frac{B_{\mathrm{AG}}}{TS_{\mathrm{conf}}(T)}, \tag{9}$$

where A_{AG} and B_{AG} are adjustable constants and $S_{\mathrm{conf}}(T)$ is the configurational entropy. Assuming that $S_{\mathrm{conf}}(T) = \Delta C_p(T - T_V)/T$, where ΔC_p is the relaxational part of the specific heat, one can see that (9) transforms into VTF (7), where $A_{\mathrm{AG}} = A_{\mathrm{VTF}}$ and $B_{\mathrm{AG}} = \Delta C_p B_{\mathrm{VTF}}/R$. The configurational entropy model of Adam and Gibbs fits a large number of viscosity data but like the free volume theory, it does not provide an accurate fit over the entire temperature range. At high and low viscosities, (9) does not describe the experimental temperature dependence of viscosity and increasingly large deviations from the experimental values are produced. In addition, the configurational entropy model gives discontinuities in the first differential of the entropy at the glass transition, despite the fact that that there are no discontinuities in experimentally measured viscosities, for example, the problem with the entropy theory is the same as for the free volume theory [43].

6.3. Avramov and Milchev Model

The Avramov and Milchev (AM) viscosity model describes the viscosity behaviour within the temperature range, where the activation energy of viscosity changes with temperature (see Figure 6). The AM model assumes that due to existing disorder, activation energy barriers with different heights occur and that the distribution function for heights of these barriers depends on the entropy. Thus, viscosity is assumed to be a function of the total entropy of the system which leads to the stretched exponential temperature dependence of equilibrium viscosity [45, 62]:

$$\ln\left[\eta(T)\right] = A_{\mathrm{AM}} + 2.3\left(13.5 - A_{\mathrm{AM}}\right)\left(\frac{T_g}{T}\right)^{\alpha}, \tag{10}$$

where in this case T_g is defined by $\ln\lfloor \eta(T_g)/(\mathrm{dPa\cdot s})\rfloor = 13.5$, A_{AM} is a constant, and α is the Avramov fragility parameter. The higher α is, the less strong is a fluid so that strong liquids have a value of α close to unity. One should note, however, that (10) fails to describe the experimental temperature dependence of viscosity in the limits of high and low temperatures.

6.4. Two-Exponential Equation

The above equations can only be used within limited temperature ranges that essentially correspond to the range of temperatures, where the activation energy for flow changes with temperature. None of them correctly describes the asymptotic low and high temperature Arrhenian viscosity behaviour [42, 43]. In addition, the nonphysical character of the fitting parameters does not give a clear understanding of changes that occur with temperature or composition. Therefore, these equations may be useful for fitting experimental measurements over limited temperature ranges, but they cannot explain the temperature dependencies of viscosity. It is well known [43, 58] that, mathematically, the viscosity of amorphous materials can most exactly be described by the two-exponential equation

$$\eta(T) = AT\exp\left(\frac{B}{RT}\right)\left[1 + C\exp\left(\frac{D}{RT}\right)\right], \tag{11}$$

where A, B, C, and D are all constants. This equation has been derived by Douglas for silicate glasses by assuming that the oxygen atoms between two silicon atoms could occupy two different positions, separated by an energy barrier [59] with flow being limited by the breaking of Si–O–Si bonds. In addition to the fact that (11) provides a very good fit to the experimental data across the entire temperature range, it correctly gives Arrhenian-type asymptotes at high and low temperatures with $Q_H = B + D$ and $Q_L = B$. For the low viscosity range ($\log(\eta/\mathrm{dPa\cdot s}) < 3$), Volf gives Q_L = 80–300 kJ/mol and for the high viscosity range $\log(\eta/\mathrm{dPa\cdot s}) > 3$ and Q_H = 400–800 kJ/mol [58]. Moreover, within narrow temperature intervals, (11) can be approximated to many types of curves, such as those given by (7) and (10). However, in contrast to them (11) gives a correct asymptotic Arrhenius-type dependence of viscosity with temperature at low and high temperatures when the activation energy of viscosity becomes constant. Equation (11) follows immediately from the Doremus conception of defect-mediated viscous flow [5, 6, 12, 47, 63, 64].

7. Defect Model of Viscous Flow

Doremus analysed data on diffusion and viscosity of silicates and suggested that diffusion of silicon and oxygen in these materials takes place by transport of SiO molecules formed on dissociation of SiO_2. Moreover, these molecules are stable at high temperatures and typically results from the vapourisation of SiO_2 [42, 43]. He concluded that the extra oxygen atom resulting from dissociation of SiO_2 leads to five-coordination of oxygen atoms around silicon. The three-dimensional (3D) disordered network of silicates is formed by $[SiO_4]$ tetrahedra interconnected via bridging oxygens $\equiv$Si•O•Si$\equiv$, where • designates a bond between Si and O, and—designates a bridging oxygen atom with two bonds •O•. The breaking out of an SiO molecule from the SiO_2 network leaves behind three oxygen ions and one silicon ion with unpaired electrons. One of these oxygen ions can bond to the silicon ion. The two other dangling bonds result in two silicon ions that are five-coordinated to oxygen ions.

Moreover, one of the five oxygen ions around the central silicon ion has an unpaired electron, and it is not bonded strongly to the silicon ion [42, 43]. Doremus suggested that this electron hole (unpaired electron) should move between the other oxygen ions similar to the resonance behaviour in aliphatic organic molecules. There is an experimental evidence for five-coordination of silicon and oxygen at higher pressures in alkali oxide SiO_2 melts from NMR, Raman, and infrared spectroscopy, and evidence for five-coordinated silicon in a $K_2Si_4O_9$ glass at atmosphere pressure [65]. Doremus concluded that in silicates, the defects involved in flow are SiO molecules resulting from broken silicon-oxygen bonds and therefore the SiO molecules and five-coordinated silicon atoms involved in viscous flow derive from broken bonds. Although he failed to reproduce the two-exponential equation of viscosity [43], it was later shown [63, 64] that (11) is a direct consequence of Doremus ideas. Indeed, assuming that viscous flow in amorphous materials is mediated by broken bonds, which can be considered as quasiparticles termed configurons [64], one can find the equilibrium concentrations of configurons $C_d = C_0 f(T)$, where $f(T) = \exp(-G_d/RT)/[1 + \exp(-G_d/RT)]$ $G_d = H_d - TS_d$ is the formation Gibbs-free energy, H_d is the enthalpy, S_d is the entropy, and C_0 is the total concentration of elementary bond network blocks or the concentration of unbroken bonds at absolute zero. The viscosity of an amorphous material can be related to the diffusion coefficient, D, of the configurons which mediate the viscous flow, via the Stokes-Einstein equation $\eta(T) = kT/6\pi rD$, where k is the Boltzmann constant and r is the radius of configuron. The probability of a configuron having the energy required for a jump is given by the Gibbs distribution $w = \exp(-G_m/RT)/[1 + \exp(-G_m/RT)]$, where $G_m = H_m - TS_m$ is the Gibbs-free energy of motion of a jumping configuron, H_m and S_m are the enthalpy and entropy of configuron motion. Thus, the viscosity of amorphous materials is directly related to the thermodynamic parameters of configurons by [5, 6, 12, 47, 63, 64]

$$\eta(T) = A_1 T\left[1 + A_2 \exp\left(\frac{B}{RT}\right)\right]\left[1 + C \exp\left(\frac{D}{RT}\right)\right] \tag{12}$$

with

$$A_1 = \frac{k}{6\pi r D_0}, \quad A_2 = \exp\left(-\frac{S_m}{R}\right), \quad B = H_m, \qquad C = \exp\left(-\frac{S_d}{R}\right), \quad D = H_d, \tag{13}$$

where $D_0 = fg\lambda^2 z p_0 \nu_0$, f is the correlation factor, g is a geometrical factor (approx. 1/6), λ is the average jump length, ν_0 is the configuron vibrational frequency or the frequency with which the configuron attempts to surmount the energy barrier to jump into a neighboring site, z is the number of nearest neighbours, and p_0 is a configuration factor.

Experiments show that, in practice, four fitting parameters usually suffice [47], indicating that viscosity is well described by (11), which follows from (12) if $A_2 \exp(B/RT) \gg 1$ (usually the case) and letting $A = A_1 A_2$. Equation (12) can be fitted to practically all available experimental data on viscosities of amorphous materials. Moreover, (12) can be readily approximated within a narrow temperature interval by known empirical and theoretical models such as VTF, AG, or the Kohlrausch-type stretched-exponential law. In contrast to such approximations, (12) can be used in wider temperature ranges and gives correct Arrhenius-type asymptotes of viscosity at high and low temperatures. Equation (12) also shows that at extremely high temperatures when $T \to \infty$, the viscosity of melts changes to a nonactivated, *for example*, non-Arrhenius behaviour, which is characteristic of systems of almost free particles.

The five coefficients A_1, A_2, B, C, and D in (12) can be treated as fitting parameters derived from the experimentally known viscosity data. Having obtained these fitting parameters, one can evaluate the thermodynamic data of configurons (e.g., network breaking defects) [47]. Hence, from known viscosity-temperature relationships of amorphous materials one can characterise the thermodynamic parameters of configurons. As the number of parameters to be found via fitting procedure is high (5 parameters when using (12) or 4 parameters when using (11)) and both equations are nonlinear, dedicated genetic algorithm was used to achieve the best fit between either (11) or (12) and experimental viscosity data [47]. An example of such evaluation is demonstrated in Figure 7, which shows the best fit for viscosity-temperature data of amorphous anorthite and diopside obtained using (12).

Calculations show that the description of experimental data using (11) is excellent with very low and uniformly scattered deviations. Although (11) provides a very good description of the viscosity data of most melts, it was found that for soda-lime silica system (mass%): $70SiO_2$ 21CaO $9Na_2O$ and B_2O_3 at very high temperatures it gives slightly, but systematically lower results compared experimental data. Thus, viscosities of these two materials at very high temperatures are better described using the complete equation (12) rather than (11) [47].

Using relationships (13) from the numerical data of evaluated parameters A_1, A_2, B, C, and D which provide the best fit of theoretical viscosity-temperature relationship (12) to experimental data, we can find enthalpies of formation and motion and entropies of formation and motion of configurons (bond system) of amorphous materials [47]. Evaluated thermodynamic parameters (enthalpies and entropies of formation and motion) of configurons in a number of amorphous materials are given in Table 4.

Data from Table 4 show that for most materials examined the entropy of configuron formation is significantly higher than the entropy of configuron motion $S_d \gg S_m$. Taking into account the values of H_m this means that $G_m/RT \gg 1$ and thus it is legitimate to simplify (12) to the simpler equation (11), that is, four fitting parameters are usually sufficient to correctly describe the viscosity-temperature behaviour of a melt. Notable exception is the SLS glass considered (mass%: $70SiO_2$ 21CaO $9Na_2O$) which, at high temperatures, exhibits deviations from (11) and requires (12) [47].

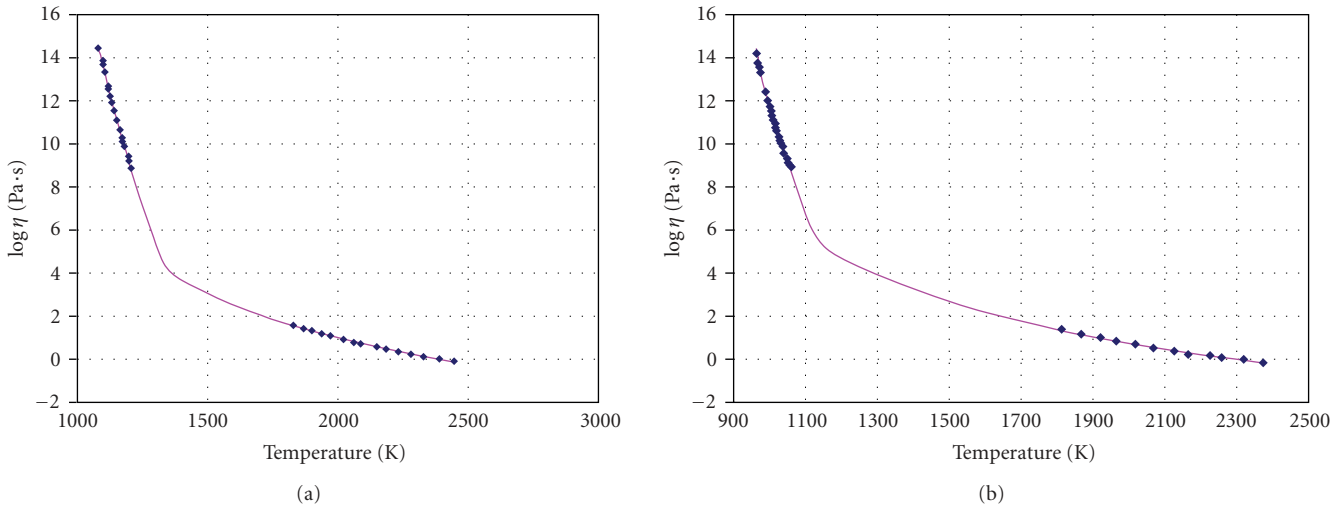

Figure 7: (a) Viscosity-temperature data for anorthite and (b) for diopside, where calculated curves were obtained using (12).

Table 4: Thermodynamic parameters of configurons.

Amorphous material	H_d/ kJ mol^{-1}	H_m, kJ mol^{-1}	S_d/R	S_m/R	S_d/S_m
Silica (SiO_2)	237	522	17.54	11.37	1.54
SLS (mass %): 70SiO_2 21CaO 9Na_2O	331	293	44.03	24.40	1.8
80SiO_2 20Na_2O	155	207	17.98	7.79	2.31
66.7SiO_2 33.3PbO	197	274	25.40	7.3	3.48
65SiO_2 35PbO	231	257	30.32	8.53	3.55
59.9SiO_2 40.1PbO	236	258	31.12	6.55	4.6
B_2O_3	258	113	44.2	9.21	4.8
65SiO_2 35Na_2O	300	186	40.71	7.59	5.36
70SiO_2 30Na_2O	258	205	34.84	5.22	5.87
75.9SiO_2 24.1PbO	262	234	36.25	5.44	6.66
Germania (GeO_2)	129	272	17.77	2.49	7.14
75SiO_2 25Na_2O	233	203	30.62	4.22	7.26
Anorthite ($CaAl_2Si_2O_8$)	884	251	79.55	0.374	213
52SiO_2 30Li_2O 18B_2O_3	420	194	52.06	0.227	229
Salol ($HOC_6H_4COOC_6H_5$)	145	118	68.13	0.114	598
α–phenyl–o–cresol	172	103	83.84	0.134	626
Diopside ($CaMgSi_2O_6$)	834	240	88.71	0.044	2016

8. Glass-Liquid Transition

Amorphous materials can be either liquid at high temperatures or solid, for example, glassy or vitreous solids at low temperatures. The transition from the glassy to the liquid state occurs at glass transition temperature. Liquid-glass transition phenomena are observed universally in various types of liquids, including molecular liquids, ionic liquids, metallic liquids, oxides, and chalcogenides [7, 31, 46, 66–68]. There is no long range order in amorphous materials, however at the liquid-glass transition a kind of freezing or transition occurs which is similar to that of second-order phase transformations and which may be possible to characterise using an order parameter. Amorphous materials (both solid, e.g., glasses and liquid, e.g., melts) can be most efficiently studied by reconstructing structural computer models and analysing coordination polyhedrons formed by constituent atoms [69]. The general theoretical description of the topologically disordered glassy state focuses on tessellations [70] and is based on partitioning space into a set of Voronoi polyhedrons filling the space of a disordered material. A Voronoi polyhedron is a unit cell around each structural unit (atom, defect, group of atoms) which contains all the points closer to this unit than to any other and is an analogue of the Wigner-Seitz cell in crystals [1–3, 70]. For an amorphous material, the topological and metric

characteristics of the Voronoi polyhedron of a given unit are defined by its nearest neighbours so that its structure may be characterised by a distribution of Voronoi polyhedrons. Considerable progress has been achieved in investigating the structure and distribution of Voronoi polyhedrons of amorphous materials using molecular dynamics (MD) models [69, 71–73]. MD simulations reveal that the difference between a liquid and glassy states of an amorphous material is caused by the formation of percolation clusters in the Voronoi network, namely, in the liquid state low-density atomic configurations form a percolation cluster whereas such a percolation cluster does not occur in the glassy state [71]. The percolation cluster made of low-density atomic configurations was called a liquid-like cluster as it occurs only in a liquid and does not occur in the glassy state. Nonetheless, a percolation cluster can be envisaged in the glassy state but formed by high-density configurations [69, 71]. Solid-like percolation clusters made of high-density configurations seem to exist in all glass-phase models of spherical atoms and dense spheres [69, 71]. Thus. MD simulations demonstrate that near T_g the interconnectivity of atoms (e.g., the geometry of bonds) changes due to the formation of percolation clusters composed of coordination Voronoi polyhedrons. While these percolation clusters made of Voronoi polyhedrons are more mathematical descriptors than physical objects, their formation results in changes in the derivative properties of materials near the T_g [69]. The liquid-glass transition is thus characterised by a fundamental change in the bond geometries so that this change can be used to distinguish liquids from glasses although both have amorphous structures [5, 6, 12, 69]. Many models were proposed to examine the transition of a liquid to glass at cooling (see overviews in [7, 26, 27, 30, 31, 43]). Table 5 outlines basic glass transition models, which are briefly discussed below.

Table 5: Basic glass transition models.

Model	Ordering process	Key concept
Free-volume	No	Change in free (excess) volume
Adam-Gibbs	No	Cooperativity of motion
Mode-coupling theory	No	Self-trapping (caging)
Kinetically constrained	No	Mobility defects
Frustration	Icosahedral ordering in glassy phase	Frustration
The Tanaka TOP	Crystallisation	Competing ordering (frustration)
Configuron percolation	Percolation cluster of broken bonds in liquid phase	Broken bond (configuron) clustering

8.1. Free-Volume Model

The free-volume model assumes that when a molecule moves by diffusion it has a certain free volume in its surroundings. The additional (free) volume becomes available above T_g in an amount given by

$$V_f = V_f(T_g) + V_g \Delta\alpha (T - T_g), \tag{14}$$

where V_g is the molar volume at T_g, $\Delta\alpha$ is the change in the volume expansion coefficient which occur at T_g [60, 74, 75]. The decrease in free volume while approaching the glass transition temperature gives an explanation for the increase of viscosity while approaching it. However, pressure dependence of the viscosity and negative dT_g/dP observed for some liquids are rather difficult to explain by this model and the validity of this assumption is questioned [27, 43, 76]. Known zero and negative values of $\Delta\alpha$ are untenable for free volume model as the free volume contraction could not explain production of relative mobile liquids above T_g.

8.2. Adam and Gibbs Model

The Adam and Gibbs model assumes that the lower the temperature is, the larger number of particles involved in cooperative rearrangements during molecular motion is, for example, the dynamic coherence length ξ of molecular motion increases with the decrease of temperature [61]. The structural relaxation time depends on the configurational entropy S_{conf} as

$$\tau_\alpha = \tau_0 \exp\left(\frac{\beta C}{S_{\text{conf}}}\right), \tag{15}$$

where τ_0 and C are constants. It is then assumed that $S_{\text{conf}}(T) = \Delta C_p (T - T_V)/T$, where ΔC_p is the relaxational part of the specific heat, T_V is the Vogel temperature, which results in VTF-type equations (see (7)). Although limited by its application, the concept of cooperativity is well describing many aspects of glass transition [27].

8.3. Mode-Coupling Model

The lower the temperature is, the higher the packing density of an amorphous material is. This leads to the stronger memory effect via mode couplings, which induces the self-trapping mechanism in the mode-coupling theory (MCT). The MCT describes this self-trapping based on a nonlinear dynamical equation of the density correlator [30, 77, 78]. The glass transition in MCT is a purely dynamic transition from an ergodic state which occurs at high temperatures to a nonergodic state at low temperatures. This transition corresponds to a bifurcation point of nonlinear equations of motion for density fluctuations when an infinite cluster of completely caged particles is formed. The transition from an ergodic to a nonergodic state occurs at the so-called mode-coupling temperature T_c, which for typical glass formers is $T_c \sim 1.2T_g$. For $T < T_c$, the density correlation function develops a nonzero value in the long-time limit (a finite value of the Edwards-Anderson-order parameter).

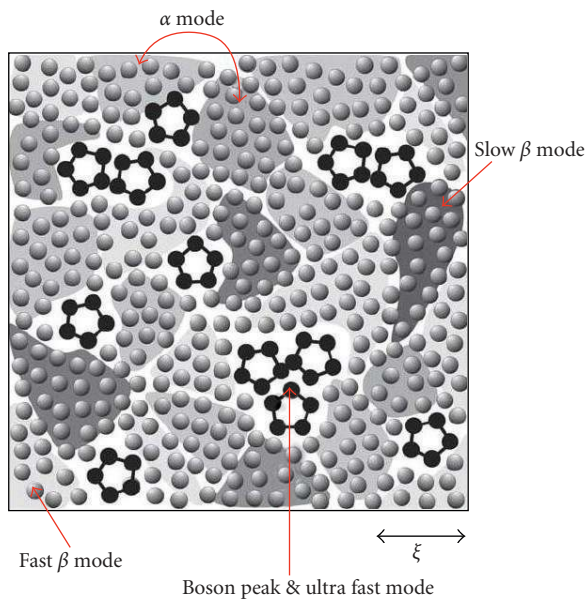

Figure 8: Schematic figure of a supercooled liquid state below melting temperature. LFS: black pentagons, NLS: grey spheres. Shaded region represents metastable islands with various degrees of crystal-like order, whose characteristic coherence length is ξ. The darker the colour is, the higher the crystal-like order and the higher the local density are [79]. Courtesy Hajime Tanaka.

The MCT describes fast β relaxation as resulting from rapid local motion of molecules trapped inside cages, while the slow process of the breakup of a cage itself leads to the α relaxation. However, analysis shows that there are no critical singularities above the glass-transition temperature in contrast to the MCT prediction [27], for example, there is no singular behaviour of viscosity at T_c. Moreover, there are no heterogeneities in MCT whereas these are observed experimentally [27]. Trap models which similarly to MCT regard the glass transition as a dynamic transition consider the distribution of the waiting time of a particle in a random potential so that particles are either trapped in cages formed by their neighbours or jump by thermal-activated rearrangements [27].

8.4. The Tanaka Two-Order-Parameter (TOP) Model

The two-order-parameter (TOP) model is based on an idea that there are generally two types of local structures in liquid: normal-liquid structures (NLSs) and locally favoured structures (LFSs). The liquid is an inhomogeneous-disordered state which has LFS created and annihilated randomly (in some cases, cooperatively) in a sea of random NLS. A supercooled liquid which is a frustrated metastable-liquid (the Griffiths-phase-like) state is in a dynamically heterogeneous state composed of metastable solid-like islands, which exchange with each other dynamically at the rate of the structural (α) relaxation time [79] (Figure 8).

Actual liquids universally have a tendency of spontaneous formation of LFS. The liquid-glass transition in TOP model is controlled by the competition between long-range density ordering towards crystallisation and short-range bond ordering towards the formation of LFS due to the incompatibility in their symmetry. Because of this, TOP model regards vitrification as phenomena that are intrinsically related to crystallisation in contrast to previous models, which regarded vitrification as a result of a homogeneous increase in the density and the resulting cooperativity in molecular motion or the frustration intrinsic to a liquid state itself. TOP model defines the calorimetric glass-transition temperature T_g as the temperature where the average lifetime of metastable islands exceeds the characteristic observation time. The mechanical and volumetric glass-transition temperature is the temperature where metastable islands, which have a long enough lifetime comparable to the characteristic observation time, do percolate [79]. The degree of cooperativity in TOP model is equal to the fraction of metastable solid-like islands, for example, TOP model operates with two states: NLS and metastable solid-like islands [79]. The metastable solid-like islands in TOP model have characteristic nm size $\sim \xi$ and are considered as resulting from random first-order transition. The lifetime of metastable islands has a wide distribution with the average lifetime equal to the structural relaxation time. The boson peak corresponds to the localised vibrational modes characteristic of the LFS and their clusters. The fast β mode results from the motion of molecules inside a cage, while the slow β mode from the rotational vibrational motion inside a cage within metastable islands.

LFSs impede crystallisation because their symmetry is not consistent with that of the equilibrium crystal. Due to random disorder effects of LFS, a liquid enters into the Griffiths-phase-like metastable frustrated state below the melting point, T_m, where its free energy has a complex multivalley structure, which leads to the non-Arrhenius behaviour of the structural relaxation. The crossover from a noncooperative to a cooperative regime TOP model describes by the fraction of the metastable solid-like islands given by the crossover function

$$f(T) = \frac{1}{\exp\left[\kappa\left(T - T_m^c\right)\right]}, \tag{16}$$

where κ controls the sharpness of transition. The NLS are favoured by density-order parameter, ρ, which increases the local density and leads to crystallisation, while the LFSs are favoured by bond-order parameter, $\overline{S}$, which results from the symmetry-selective parts of the interactions and increases the quality of bonds. The average fraction of LFS ($\overline{S}$) is given by

$$\overline{S} \cong \left(\frac{g_S}{g_\rho}\right) \exp\left[\beta(\Delta E - P\Delta v)\right], \tag{17}$$

where $\beta = 1/k_B T$, k_B is the Boltzmann constant, P is the pressure, ΔE and Δv are the energy gain and the volume change upon the formation of an LFS, g_S and g_ρ are the degrees of degeneracy of the states of LFS and NLS, respectively. It is assumed that $g_S \gg g_\rho$ and $\Delta E > 0$. Δv can be

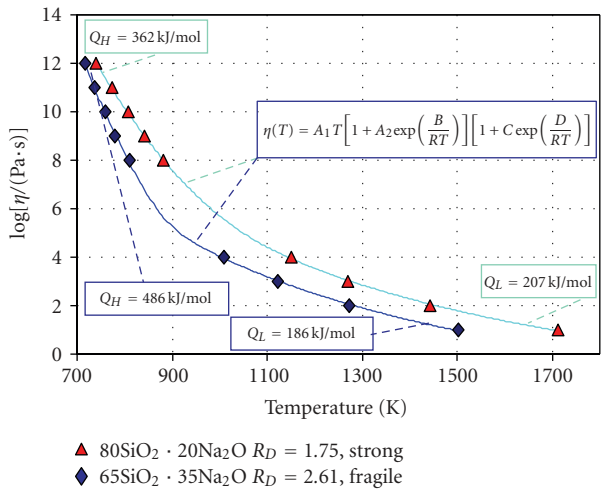

Figure 9: Viscosity of two SiO_2–Na_2O systems.

either positive or negative depending upon material, for example, $\Delta v > 0$ for liquids with tetrahedral units. NLSs have many possible configurations as well as various bonding states compared with the unique LFS and there is a large loss of entropy upon the formation of an LFS, which is given by

$$\Delta\sigma = k_B \ln\left(\frac{g_S}{g_\rho}\right). \tag{18}$$

NLS is a short-lived random structure whereas LFS a long-lived rigid structural element. The lifetime of an LFS can be estimated as

$$\tau_{\mathrm{LFS}} = \tau_\alpha^0 \exp\left(\beta\Delta G_S\right), \tag{19}$$

where τ_α^0 is the structural relaxation time of NLS and ΔG_S is the energy barrier to overcome upon the transformation from an LFS to an NLS.

TOP model defines fragility by fraction of LFS: the larger the $\overline{S}$ is, the stronger (less fragile) the liquid is. An example of conclusion drawn from TOP model is the increases the fragility of SiO_2 upon the addition of Na_2O, for example, the higher the Na_2O content is, the higher the fragility which conforms the experimental data is (see Figure 9). Na_2O acts as a network modifier breaking the Si–Si links via bridging oxygens. Tanaka proposed that Na_2O destabilises the LFS, for example, that Na_2O is the breaker of LFS, probably, the 6-member ring structures of SiO_2. Since Na_2O reduces the number density of LFS ($\overline{S}$), it increases the fragility of SiO_2 and weaken the boson peak [80].

LFSs impede crystallisation because their symmetry is not consistent with that of the equilibrium crystal. A similar idea was exploited by Evteev et al. to explain vitrification of amorphous metals [69, 81]. In addition, strong liquids should be more difficult to crystallise than fragile below T_g [82].

8.5. Frustration Models

Local energetically preferred structures over simple crystalline packing impede crystallisation because their symmetry is not consistent with that of the equilibrium crystal, for example, frustrated over large distance. Frustration models assume that the glass transition is a consequence of the geometric frustration [83–86]. Typically, icosahedron is the most compact and stable from the energy point of view among all coordination polyhedrons encountered in both ordered and disordered densely packed structures such as amorphous metals. For example, Kivelson et al. [85, 86] considered frustration of an icosahedral structure which is the low-symmetry reference state, into which a liquid tends to be ordered, and ascribed the glass transition to an avoided critical point of a transition between a liquid and an ideal icosahedral structure. The Hamiltonian used, for example, in [85, 86] was similar to that of Steinhardt et al. [84]

$$H = -J_S \sum_{i,j} \vec{S}_i \cdot \vec{S}_j + \frac{K_S \sum_{i \neq j} \vec{S}_i \cdot \vec{S}_j}{\left|\vec{R}_i - \vec{R}_j\right|}, \tag{20}$$

where J_S and K_S are both positive. The first term which is a short-range ferromagnetic interaction favours long-range order of the locally preferred structure, while the second term which is a long-range antiferromagnetic interaction is responsible for the frustration effects. The ordering is thus prevented by internal frustration of the order parameter itself as in other frustration models.

Using MD simulations, Evteev et al. [69] showed that in the process of fast cooling of melt iron, the fraction of atoms for which the coordination polyhedron is an icosahedron (the Voronoy polyhedron is a dodecahedron) increases most intensely. Moreover, formation of a percolation cluster from mutually penetrating and contacting icosahedrons with atoms at vertices and centres provides stabilisation of the amorphous phase and impedes crystallisation during fast cooling of Fe from melt [69, 81]. Evteev et al. showed that glassy phase forms at the glass transition temperature based on a percolation cluster of mutually penetrating icosahedrons contacting one another, which contain atoms at the vertices and at the centres (Figure 10). A fractal cluster of icosahedrons incompatible with translational symmetry plays the role of binding carcass hampering crystallisation and serves as the fundamental basis of structural organisation of the glassy (solid amorphous state) of iron, which basically distinguishes it from the melt.

8.6. Kinetically Constrained Models

Kinetically constrained models consider slow dynamics as of a purely kinetic origin [27, 87], where dynamical constraints appear below a crossover temperature T_o or above a corresponding packing fraction, so that above T_o the dynamics is liquid-like whereas below T_o the dynamics becomes heterogeneous. Hunt, for example, defined the glass as a supercooled liquid, whose time scale required for equilibration is a percolation relaxation time and derived the glass transition temperature from equalising the relaxation

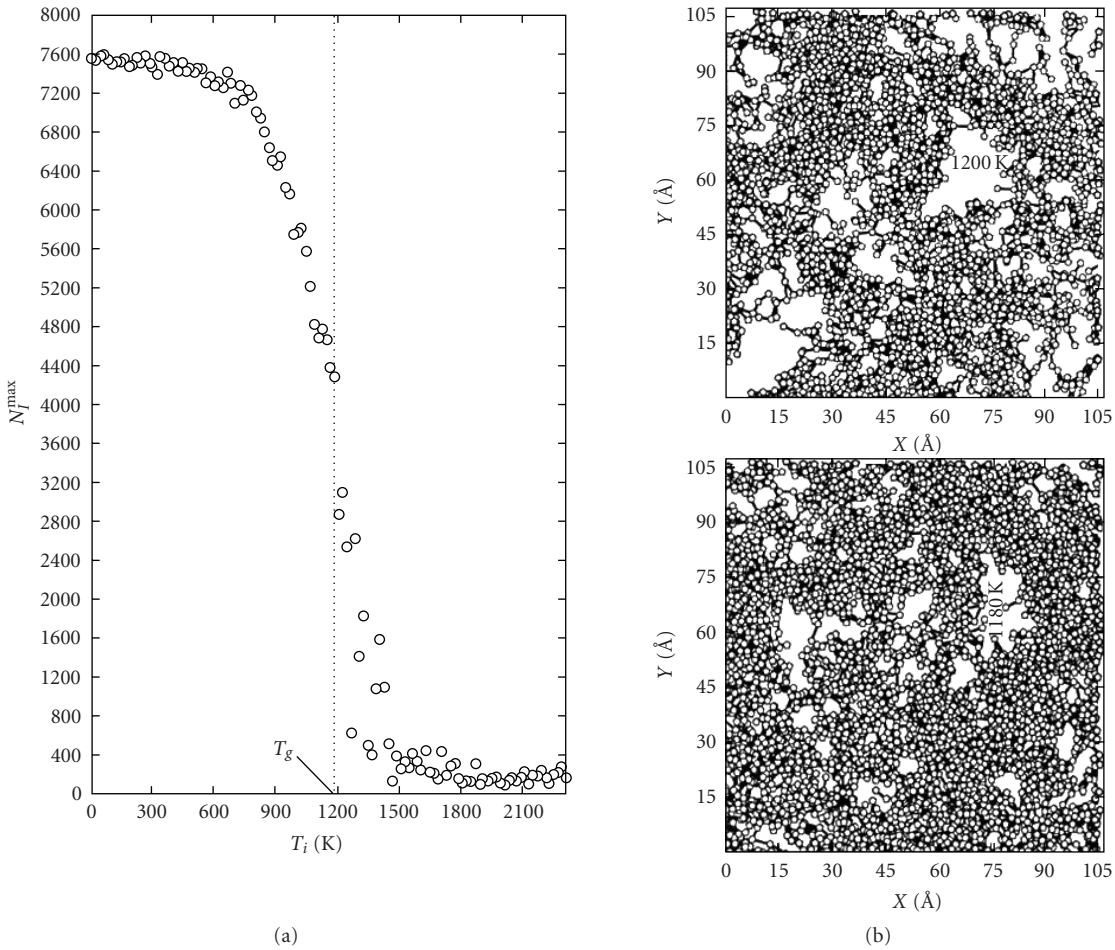

Figure 10: The structure of amorphous iron resulting from molecular dynamics simulations [69]. (a) The size of the largest cluster formed by clustered icosahedrons with the temperature T_i. (b) Projections of the largest cluster formed by clustered icosahedrons onto one of the faces of the computational cell at temperatures 1200 K (*2*) and 1180 K (*5*). Courtesy Alexander Evteev.

time τ_c to the experimental time taken arbitrary as $t_{\text{exp}} = 100$ seconds [88]. The Hunt equation

$$T_g \cong \frac{E_m}{18k_B} \tag{21}$$

relates the glass transition temperature T_g with the peak energy in the distribution of hoping barrier heights E_{ij} of individual relaxation processes

$$\tau_{ij} = \nu_{\text{ph}}^{-1} \exp\left(\frac{E_{ij}}{k_B T}\right), \tag{22}$$

where ν_{ph} is a typical vibrational frequency roughly 10^{12} Hz. Using the Coulomb attraction between opposite charges and Lennard-Jones repulsive interaction, Hunt obtained an estimation for E_m:

$$E_m \approx \frac{qq'}{4\pi\varepsilon_0\varepsilon r_0}, \tag{23}$$

where q and q' are ionic charges, r_0 is the equilibrium interionic distance minimising the interaction potential, and ε is the macroscopic dielectric constant. Accounting that on pressure application the internal pressure changes to

$$U = -\frac{qq'}{4\pi\varepsilon_0\varepsilon r} + \left(\frac{qq'}{48\pi\varepsilon_0\varepsilon r_0}\right)\left(\frac{r_0}{r}\right)^{12} + P\left(r^3 - r_0^3\right), \tag{24}$$

where P is pressure, Hunt obtained an excellent description of pressure dependence of the glass transition temperature $T_g(P)$ in ionic liquids [76, 89]. Moreover, this approach gave an explanation of reduced glass transition temperature by confinement in small pores [90]:

$$T_g(\infty) - T_g(L) = a\left(\frac{l}{L}\right), \tag{25}$$

where a is a constant, l is a typical hopping length, and L is the pore size. In addition, Hunt explained application of Ehrenfest theorems to the glass transition [91].

8.7. Configuron Percolation Model

In contrast to other models based on percolation theory, the configuron percolation model of glass transition considers

the percolation not via atoms or bonds, but the percolation via broken bonds. For example, the configuron percolation model examines not the transition from the liquid to the glass on decrease of temperature, but the transition from the glass to liquid on temperature increase. The transition of a liquid to a glass has many features of second-order phase transition. Second-order phase transformations are characterised by symmetry change. The translation-rotation symmetry in the distribution of atoms and molecules is deemed unchanged at the liquid-glass transition, which retains the topological disorder of fluids. What kind of symmetry is changed at glass-liquid transition? To answer to this question, it is expedient to consider the distribution of configurons (broken bonds) instead of atoms and to focus the attention on topology of broken bonds at glass-liquid transition [5, 6, 12, 47]. Consider an ideal disordered network representing an oxide system such as amorphous SiO_2 or GeO_2. Using the Angell bond lattice model [92], one can represent condensed phases by their bond network structures. Thus, one can focus the attention on temperature changes that occur in the system of interconnecting bonds of a disordered material rather than of atoms. In this approach, the initial set of N strongly interacting cations such as Si^{+4} or Ge^{+4} is replaced by a congruent set of weakly interacting bonds of the system. The number of bonds will be $N_b = NZ$, where Z is the coordination number of cations, for example, $Z = 4$ for SiO_2 and GeO_2. For amorphous materials which have no bridging atoms such as amorphous Fe, Si, or Ge, $N_b = NZ/2$. Figures 11(a) and 11(b) illustrate schematically the replacement of a disordered atomic structure by the congruent bond structure.

At absolute zero temperature $T = 0$, there are no broken bonds (Figure 11(b)), however at any finite temperature T, there are thermally activated broken bonds, for example, configurons (Figure 11(c)). Compared with a crystal lattice of the same material, the disordered network typically contains significantly more point defects such as broken bonds or vacancies. For example, the relative concentration of vacancies in crystalline metals just below the melting point is only 10^{-3}-10^{-4} [2, 93]. The energetics of the disordered net are weaker and point defects can be formed more easily than in crystals of the same chemical composition. The difference appears from the thermodynamic parameters of disordered networks. The formation of configurons is governed by the formation of Gibbs-free energy G_d. Temperature-induced formation of configurons in a disordered covalent network can be represented by a reaction involving the breaking of a covalent bond, for example, in amorphous silica:

$$\equiv \mathrm{Si} \bullet \mathrm{O} \bullet \mathrm{Si} \equiv \xrightarrow{T} \equiv \mathrm{Si} \circ \mathrm{O} \bullet \mathrm{Si} \equiv . \tag{26}$$

Figure 12 illustrates the formation of a configuron in the amorphous SiO_2. Breaking of a covalent bond is followed by relaxation effects which lead to the formation of a relaxed or equilibrium configuron. As pointed out by Doremus [42, 43], relaxation effects after the breaking of the bond result in five-coordinated silicon ions.

The higher the temperature is, the higher the concentration of thermally created configurons is. Because the system of bonds has two states, namely, the ground state corresponding to unbroken bonds and the excited state corresponding to broken bonds, it can be described by the statistics of two-level systems and the two states of the equivalent system are separated by the energy interval G_d governing (27) [64]. The statistics of two level systems leads to the well-known relationship for equilibrium concentrations of configurons C_d and unbroken bonds C_u [64, 94]

$$C_d = C_0 f(T), \qquad C_u = C_0[1 - f(T)],$$
$$f(T) = \frac{\exp(-G_d/RT)}{[1 + \exp(-G_d/RT)]}, \tag{27}$$

at absolute zero temperature $C_u(0) = C_0$. The concentration of configurons gradually increases with the increase of temperature, and at $T \to \infty$ achieves its maximum possible value $C_d = 0.5\,C_0$ if $G_d > 0$. At temperatures close to absolute zero, the concentration of configurons is very small $f(T) \to 0$. These are homogeneously distributed in the form of single configurons in the disordered bond network. Configurons motion in the bond network occurs in the form of thermally activated jumps from site to site and in this case all jump sites are equivalent in the network. The network, thus, can be characterised as an ideal 3D-disordered structure which is described by an Euclidean 3D geometry. As the temperature increases, the concentration of configurons gradually increases. The higher the temperature is, the higher the concentration of configurons and, hence, some of them inevitably will be in the vicinity of others. Two and more nearby configurons form clusters of configurons and the higher the concentration of configurons is, the higher the probability of their clustering is (Figure 11(d)). Although configuron clusters are dynamic structures, the higher the temperature is, the larger are clusters made of configurons in the disordered bond network. As known from the percolation theory, when the concentration of configurons exceeds the threshold level, they will form the macroscopic so-called percolation cluster, which penetrates the whole volume of the disordered network [95]. The percolation cluster made of broken bonds forms at glass transition temperature and grows in size with the increase of temperature.

The configurons are moving in the disordered network, therefore, the percolation cluster made of broken bonds is a dynamic structure which changes its configuration remaining, however, an infinite percolation cluster. The percolation cluster is made entirely of broken bonds and hence is readily available for a more percolative than a site-to-site diffusive motion of configurons. Hence, above the percolation level the motion of configurons in the bond network occurs via preferred pathways through the percolation cluster. The percolation cluster near the percolation threshold is fractal in dimension, therefore the bond system of an amorphous material changes its Hausdorff-Besikovitch dimensionality from Euclidian 3 below the T_g (where the amorphous material is solid), to fractal 2.55 ± 0.05 above the T_g, where the amorphous material is liquid [5, 6, 12].

As the bond network of an amorphous material is disordered, the concentration of configurons at which the

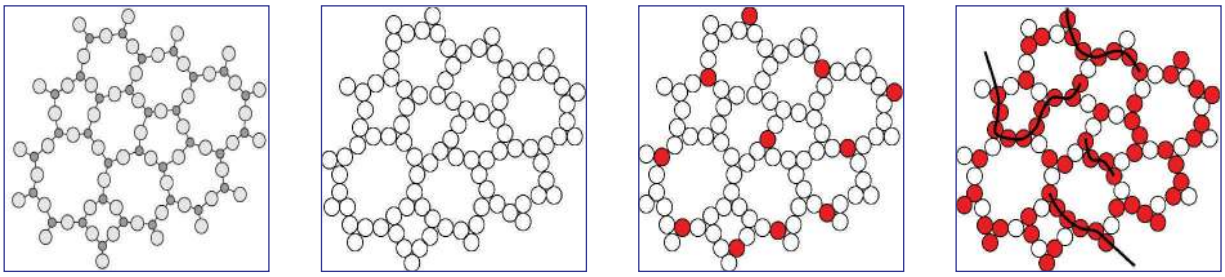

(a) $T = 0$ (b) $T = 0$ (c) $T_1 > 0$ (d) $T_2 > T_1$

Figure 11: Schematic of disordered bond lattice model of an amorphous material: (a) distribution of atoms in amorphous phase at $T = 0$; (b) distribution of bonds in amorphous phase at $T = 0$; (c) distribution of bonds in amorphous phase at $T_1 > 0$; (d) distribution of bonds in amorphous phase at higher temperatures $T_2 > T_1$ when configuron clustering occurs.

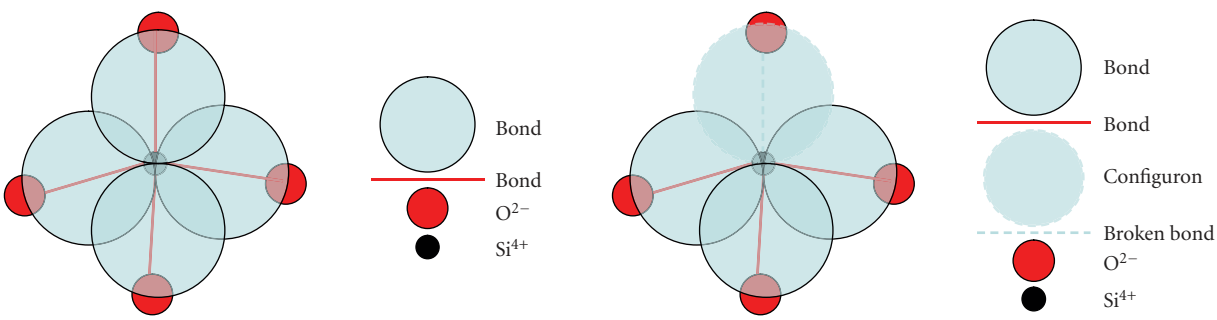

(a) (b)

Figure 12: (a) Schematic of 4 covalent bonds (b) and one broken bond in SiO_2.

percolation threshold is achieved can be found using the universal critical percolation density f_c, which remains the same for both ordered and disordered lattices [95, 96]. The relative concentration of broken bonds is given by $f(T) = C_d/C_0$ which shows that the higher the temperature is, the higher is $f(T)$. Assuming that at $C_d/C_0 = 1$ the space is completely filled by configurons, one can designate $f(T)$ as the volume fraction of space occupied by configurons. Thus, the critical (glass-transition) temperature T_g at which the percolation threshold is achieved can be found assuming that the configurons achieve the universal critical density given by the percolation theory

$$f(T_g) = f_c. \tag{28}$$

For SiO_2 and GeO_2, it was supposed that $f_c = \vartheta_c$, where ϑ_c is the Scher-Zallen critical density in the 3D space $\vartheta_c = 0.15 \pm 0.01$ [95–97]. For many percolating systems, the value of f_c is significantly lower compared to ϑ_c [96].

At temperatures above T_g, the space is filled by configurons at concentrations which exceed the critical density f_c, therefore they form the percolation cluster with fractal geometry changing the state of material from solid-like (glass) to liquid-like. This leads to the following equation of glass transition temperature [5, 6, 12]:

$$T_g = \frac{H_d}{[S_d + R\ln[(1 - f_c)/f_c]]}. \tag{29}$$

Note that because $S_d \gg R$, this equation can be simplified to $T_g \approx H_d/S_d$, which is an analogue of the Diennes ratio used to assess the melting temperatures of crystalline solids. Below the T_g, the configurons are uniformly distributed in space, and formation of clusters is improbable. The geometry of network defects in this area can be characterised as 3D Euclidean. With the increase of temperature at $T = T_g$, the concentration of defects achieves the critical concentration for formation of a percolation cluster. Above the T_g, a percolation cluster made of configurons is formed, and the geometry of the network becomes fractal with the fractal dimension 2.55 ± 0.05 near the T_g.

Equation (29) gives excellent data for glass-transition temperatures [5, 6, 12, 47]. Note that the glass-transition temperature (29) depends on thermal history for several reasons: (i) during cooling, a part of material is inevitably crystallised, (ii) configurons need a certain time to relax to their equilibrium sizes, and (iii) the enthalpy of configuron formation depends on the overall state of amorphous material including its quenched density which can be assessed from [62] $H_d \approx q_1 q_2 e^2/\varepsilon d_a N$, where q_z is the valence of the cation-anion pair, e is the standard unit of charge, d_a is the average bond distance, N is the coordination number, and ε is the dielectric constant of the glass which depends on the thermal history. This estimation is similar to the Hunt assessment (24) [89].

The characteristic linear scale which describes the branch sizes of dynamic clusters formed by configurons is the

correlation length $\xi(T)$. Below the T_g, the correlation length gives characteristic sizes of clusters made of configurons whereas above the T_g, it shows characteristic sizes of clusters made of unbroken bonds, for example, atoms. $\xi(T)$ gives the linear dimension above which the material is homogeneous, for example, a material with sizes larger than $\xi(T)$ has on average uniformly distributed configurons. At sizes smaller compared to $\xi(T)$, the amorphous material is dynamically inhomogeneous, for example, has a fractal geometry [95, 96]. Because of the formation of percolation cluster, the material has a fractal geometry at lengths smaller than $\xi(T)$. It means that the glass loses at glass-liquid transition the invariance for the Euclidian space isometries such as translation and rotation on length scales smaller than $\xi(T)$. The liquid near the glass transition is dynamically inhomogeneous on length scales smaller than $\xi(T)$ and remains unchanged for fractal space group of isometries. Figure 13 shows schematically the structure of an amorphous material near the glass transition temperature.

The fractal dimension of percolation clusters near the percolation threshold is $d_f = 2.55 \pm 0.05$. At temperatures far from T_g, the correlation length is small, whereas at temperatures approaching T_g, it diverges

$$\xi(T) = \frac{\xi_0}{|f(T) - f_c|^{\nu}}, \tag{30}$$

where the critical exponent $\nu = 0.88$ [93, 94].

If sample sizes are smaller than $\xi(T)$, the amorphous material is dynamically inhomogeneous and has a fractal geometry. Finite size effects in the glass transition are described as a drift to lower values of T_g; when sample sizes L decrease [6],

$$T_g(\infty) - T_g(L) = 0.1275 T_g \left(\frac{RT_g}{H_d}\right)\left(\frac{\xi_0}{L}\right)^{1.136}, \tag{31}$$

one can see that this expression conforms well with (25), for example, with the Hunt results [90]. The heat capacity per mole of configurons involved in the percolation cluster near T_g was found as [6, 12]

$$C_{p,\mathrm{conf}} = R\left(\frac{H_d}{RT}\right)^2 f(T)[1 - f(T)] \times \left(1 + \frac{\beta P_0 (\Delta H/H_d) T_1^{1-\beta}}{|T - T_g|^{(1-\beta)}}\right), \tag{32}$$

where $T_1 = RT_g^2/\theta_c(1 - \theta_c)H_d$, $\beta = 0.41$ is the critical exponent [95, 96], P_0 is a numerical coefficient close to unity, for example, for strong liquids $P_0 = 1.0695$, and $\Delta H \ll H_d$ is the enthalpy of configurons in the percolation cluster.

The configuron model of glass transition shows that the linear expansion coefficient near the T_g behaves as [6]

$$\alpha_{\mathrm{conf}} = N_b\left(\frac{\Delta V_0 H_d}{VRT^2}\right) f(T)[1 - f(T)] \times \left(1 + \frac{\beta P_0 (\Delta H/H_d) T_1^{1-\beta}}{|T - T_g|^{(1-\beta)}}\right), \tag{33}$$

Table 6: Glass transition temperatures of amorphous materials.

Amorphous material	R_D	T_g/K	f_c
Silica (SiO_2)	1.45	1475	0.15
Germania (GeO_2)	1.47	786	0.15
SLS (mass%): $70SiO_2$ $21CaO$ $9Na_2O$	2.16	870	1.58×10^{-3}
B_2O_3	3.28	580	9.14×10^{-5}
Diopside ($CaMgSi_2O_6$)	4.51	978	6.35×10^{-7}
Anorthite ($CaAl_2Si_2O_8$)	4.52	1126	3.38×10^{-7}

where $\Delta V_0/V$ is the relative change of volume per one broken bond. One can observe, hence, that both thermal expansion coefficient and heat capacity show divergences near T_g proportional to $\propto 1/|T - T_g|^{0.59}$ [6, 12] (see Figure 1).

Complex oxide systems are typically fragile. These are described by a modified random network model comprising network modifying cations distributed in channels, and the value of f_c in these systems is significantly lower compared to strong materials as can be seen from Table 6 [47].

Data from Table 6 show that the higher the fragility ratio is, the lower the threshold for the formation of percolation clusters of configurons in the material is. There is a direct anticorrelation between the fragility ratio and configuron percolation threshold which determines the glass transition temperature. Networks that exhibit only small changes in the activation energy for flow with temperature form percolation clusters of configurons at the classical Scher-Zallen critical density. In contrast, fragile liquids, which are characterised by a higher density of configurational states, have a very low percolation threshold which decreases with increasing fragility.

Angell interpreted strong and fragile behaviours of liquids in terms of differences in topology of the configuration space potential energy hypersurfaces [55]; for example, fragile liquids have a higher density of configurational states and hence a higher degeneracy leading to rapid thermal excitations. In the bond lattice model of amorphous materials, the system of strongly interacting ions is replaced by a congruent set of weakly interacting bonds. The glass transition is related in this model with formation of percolation clusters made of configurons and change of bond Hausdorff-Besikovitch dimension [5, 6]. The diminishing values of configuron percolation thresholds can be interpreted in terms of configuron size or delocalisation. It is deemed that in fragile liquids the configurons are larger, for example, delocalised; moreover, the higher the fragility ratio is, the larger the effective configuron radius and its delocalisation are. Due to configuron delocalisation, the glass transition, which is associated with the increase of bond Hausdorff-Besikovitch dimension from $d_f = 2.55 \pm 0.05$ to 3, occurs in fragile liquids at lower percolation threshold compared to strong liquids. The effective configuron radius, r_c, can be assessed from

$$r_c = r_d\left(\frac{\vartheta_c}{f_c}\right)^{1/3}, \tag{34}$$

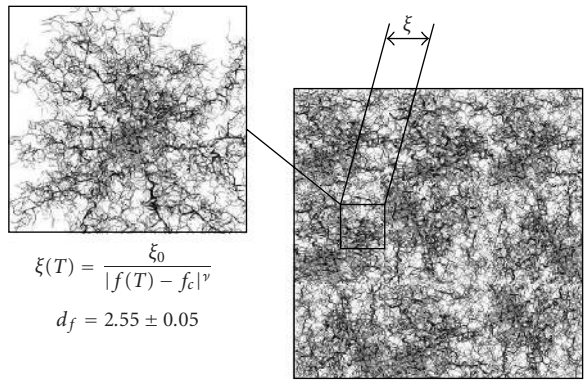

Figure 13: Schematic representation of the dynamic homogeneous fractal structure of an amorphous material near the glass transition temperature. Below the T_g, the correlation length gives characteristic sizes of clusters made of configurons, whereas above the T_g, it shows characteristic sizes of clusters made of unbroken bonds. The higher the temperature is, the smaller sizes of fractal volumes are. Note that the structure shown is dynamical, for example, changes with time due to configuron diffusion.

where r_d is the bond radius (half of bond length). For strong liquids, $f_c = \vartheta_c$ and thus the configuron radii are equal to bond radii. Strong materials such as silica have small radii configurons localised on broken bonds and because of that they should show a smaller dependence on thermal history which conforms to experimental findings [98]. In fragile materials, the effective configuron radii considerably exceed bond radii, $r_c \gg r_d$. For example, B_2O_3 with fragility ratio $R_D = 3.28$ has $r_c = 11.79 r_d$, which is due to its specific structure. Both crystalline and vitreous boron oxides consist of planar oxygen triangles centred by boron most of which accordingly to X-ray diffraction data are arranged in boroxol rings (see [7]). The two-dimensional nature of the B_2O_3 network means that the third direction is added by crumbling of the planar structures in a three-dimensional amorphous boric oxide which result in effective large size configuron compared to bond length.

9. Ordering at Glass-Liquid Transition

Because of the formation of percolation cluster at glass-liquid transition, the amorphous material looses the invariance for the Euclidian space isometries such as translation and rotation on length scales smaller than $\xi(T)$, for example, at these length scales, it is dynamically inhomogeneous. The percolation cluster is also called an infinite cluster as it penetrates the whole volume of material which as a result drastically changes its physical properties from solid-like below to fluid-like above the percolation threshold. The geometry of a percolation cluster near the percolation threshold is fractal with the Hausdorff-Besikovitch dimension $d_f = d - \beta/\nu$, where β and ν are critical exponents (indexes) and $d = 3$ is the dimension of the space occupied by the initial-disordered network, so that $d_f = 2.55 \pm 0.05$. The formation of percolation cluster changes the topology of bonds network from the 3D Euclidean below to the fractal d_f-dimensional above the percolation threshold. At glass-liquid transition, the amorphous material changes the group of isometries from the Euclidian to the fractal space group of isometries at length scales smaller than $\xi(T)$. An amorphous material is represented by a disordered bond network at all temperatures, however it has a uniform 3D distribution of network breaking defects at low concentrations in the glassy state and a fractal d_f-dimensional distribution at high enough temperatures when their concentration exceeds the percolation threshold in the liquid state. Although on average the liquids are homogeneous, they are dynamically inhomogeneous on length scales smaller than $\xi(T)$ near the glass transition. Changes that occur in the geometries of amorphous material at T_g affect their mechanical properties. Above T_g, the geometry is fractal like in liquids [73] and the mechanical properties are similar to those of liquids. The structure of material remains disordered at all temperatures although the space distribution of configurons as seen above is different below and above the percolation threshold changing the geometry from the Euclidean to fractal.

Although, to a certain extent, being disordered at all temperatures, the bond structure above the percolation threshold becomes more ordered as a significant fraction of broken bonds, for example, configurons belong to the percolation cluster. The density of the percolation cluster of configurons, φ, can serve as the order parameter [6, 99] and for the liquid phase it has nonzero values, whereas for the glassy phase, $\varphi = 0$ (Figure 14).

Second-order phase transitions in ordered substances are typically associated with a change in the crystal lattice symmetry, and the symmetry is lower in the ordered phase than in the less ordered phase [98]. In the spirit of the Landau ideas, the transition from a glass to a liquid spontaneously breaks the symmetry of bonds, for example, of the configuron system. At glass-liquid transition, the amorphous material changes the group of isometries from the Euclidian to the fractal space group of isometries at length scales smaller than $\xi(T)$. The description of a second-order phase transition as a consequence of a change in symmetry is given by the Landau-Ginzburg theory [100]. The order parameter φ, which equals zero in the disordered phase and has a finite value in the ordered phase, plays

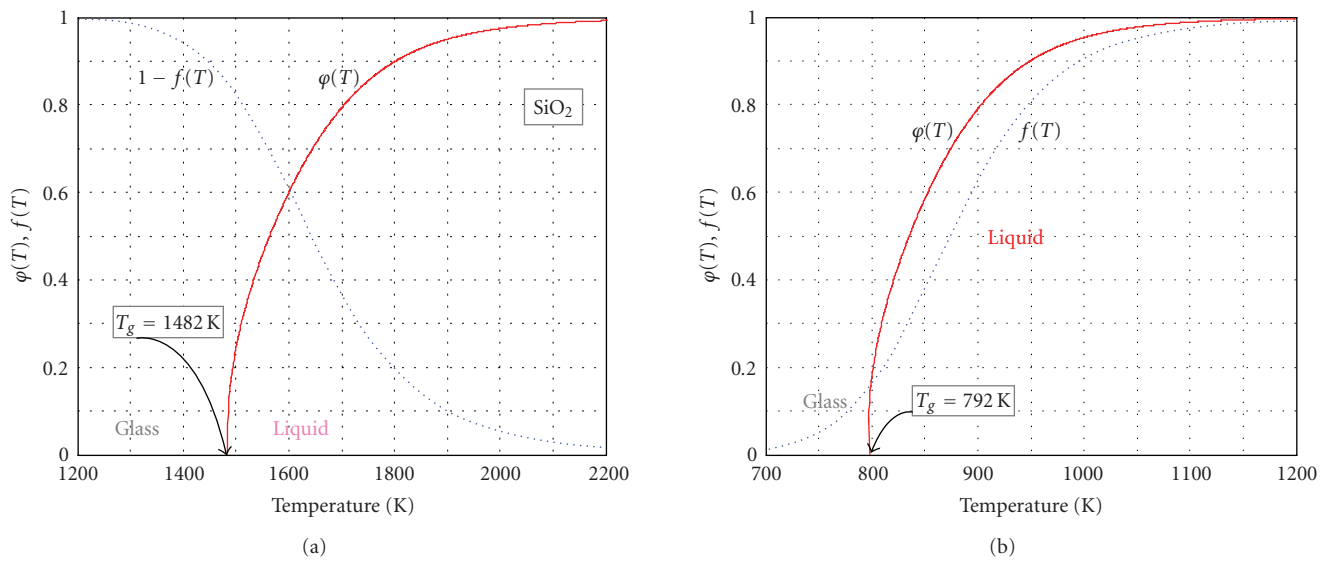

Figure 14: Temperature dependence of the order parameter of configurons in (a) amorphous SiO_2 (b) and GeO_2 [6]. The liquid phase seems more ordered for configurons (broken bonds) which are largely a part of the percolation cluster in the liquid whereas in the glassy phase the configurons are randomly distributed in the solid.

an important role in the theory of second-order phase transitions. For a glass-liquid transition, as well as in the general case of percolation phase transitions, the density of the percolation cluster of configurons is an order parameter [6].

Crystalline materials are characterised by 3D Euclidean geometries below their melting point T_m. Thus, both glasses below T_g and crystals below T_m are characterised by the same 3D geometry. Glasses behave like isotropic solids and are brittle. Because of the 3D bond geometry, glasses break abruptly and the fracture surfaces of glasses typically appear flat in the "mirror" zone. Glasses change their bond geometry at T_g. When melting occurs, the geometry of crystalline materials also changes, as revealed by MD experiments to fractal structure with $d_f \approx 2.6$ [73]. It is also known that emulsion particles have homogeneous fractal distribution in liquids and the fractal dimension of emulsions is $d_f = 2.5 \pm 0.1$ [101]. With the increase of temperature, the clusters of configurons grow in size whereas clusters of atoms decrease their sizes. Further changes in the dimensionality of bond structure can occur. Finally, when no unbroken bonds remain in the system, the material is transformed to a gaseous state. Therefore, for the system of bonds the phase changes can be represented by the consequence of changes of the Hausdorf dimension $d = 3$ (solid) $\rightarrow$ $d_f = 2.55 \pm 0.05$ (liquid) $\rightarrow$ $d = 0$ (gas).

10. Conclusions

Amorphous materials can occur either in liquid or glassy state. Amorphous materials are largely spread in the nature both in form of melts and glasses, for example, it has been found that the inner core of Earth is in a disordered, for example, glassy form [102] (see also [103]). The transition from the liquid to the glassy state evidences characteristic discontinuities of derivative thermodynamic parameters such as the coefficient of thermal expansion or the specific heat. The analysis of bonding system of glassy and crystalline materials shows that they both hold the same Hausdorff dimension of bonds $d = 3$. The similarity in bonding of both glassy and crystalline materials means the similarity of their behaviour in many aspects such as the propagation of acoustic signals which revealed the solid state of the Earth core.

Amorphous materials are liquid above the glass-transition temperature. The configuron model of glass transition shows that the transition of amorphous materials from glassy to liquid state is a percolation-type phase transition. The bonding system of an amorphous material changes its geometry from 3D in the glassy state to fractal one ($d_f = 2.55 \pm 0.05$) in the liquid state due to formation of infinite size dynamic percolation clusters made of broken bonds—configurons. The configuron model of glass transition gives an explicit equation of glass-transition temperature (29) and demonstrates characteristic jumps in specific heat and thermal expansion. The higher the concentration of broken bonds is, the lower the viscosity is, which is a continuous function of temperature both for glassy and liquid amorphous materials and has no discontinuities at glass transition. The defect model of viscosity results in a universal viscosity (12) valid at all temperatures. Table 7 summarises temperature changes of states, geometry of bonds, and viscosity of amorphous materials.

Transitions in disordered media from glassy to liquid states are universal and reflect changes in the bonding system. Because of that, the configuron model of glass transition can be used to provide insights on embrittlement of materials composed of microcrystals at low temperatures

Table 7: Viscosity and bond geometries of amorphous materials.

Temperature	$T < T_g$	$T > T_g$
State	Solid (glassy)	Liquid (melt)
The Hausdorff dimension of bonds	$d = 3$	$d_f = 2.55 \pm 0.05$
Viscosity	Continuous decreasing function of temperature	
	Activation energy high	Activation energy low

as well as on such natural phenomena as quick sand formation. In all such cases, formation of additional bonds between elementary particles which constitute the material, for example, microcrystals or sand grains leads to their solid-like behaviour at lower temperatures or denser packing.

References

[1] N. W. Ashcroft and N. D. Mermin, *Solid State Physics*, Holt-Sauders, Tokyo, Japan, 1976.

[2] C. Kittel, *Introduction to Solid State Physics*, John Wiley & Sons, New York, NY, USA, 1996.

[3] A. R. West, *Basic Solid State Chemistry*, John Wiley & Sons, Chichester, UK, 1999.

[4] C. A. Angell, "Glass-formers and viscous liquid slowdown since David turnbull: enduring puzzles and new twists," *MRS Bulletin*, vol. 33, no. 5, pp. 544–555, 2008.

[5] M. I. Ojovan, "Glass formation in amorphous SiO_2 as a percolation phase transition in a system of network defects," *JETP Letters*, vol. 79, no. 12, pp. 632–634, 2004.

[6] M. I. Ozhovan, "Topological characteristics of bonds in SiO_2 and GeO_2 oxide systems upon a glass-liquid transition," *Journal of Experimental and Theoretical Physics*, vol. 103, no. 5, pp. 819–829, 2006.

[7] A. K. Varshneya, *Fundamentals of Inorganic Glasses*, Society of Glass Technology, Sheffield, UK, 2006.

[8] D. E. Clark and B. K. Zoitos, Eds., *Corrosion of Glass, Ceramics and Ceramic Superconductors*, William Andrew/Noyes, Norwich, NY, USA, 1992.

[9] M. I. Ojovan and W. E. Lee, *An Introduction to Nuclear Waste Immobilisation*, Elsevier Science, Amsterdam, The Netherlands, 2005.

[10] The International Commission on Glass, November 2007, http://www.icg.group.shef.ac.uk.

[11] A. D. McNaught and A. Wilkinson, Eds., *The IUPAC Compendium on Chemical Terminology*, Royal Society of Chemistry, Cambridge, UK, 1997.

[12] M. I. Ojovan and W. E. Lee, "Topologically disordered systems at the glass transition," *Journal of Physics Condensed Matter*, vol. 18, no. 50, pp. 11507–11520, 2006.

[13] M. Telford, "The case for bulk metallic glass," *Materials Today*, vol. 7, no. 3, pp. 36–43, 2004.

[14] W. H. Wang, C. Dong, and C. H. Shek, "Bulk metallic glasses," *Materials Science and Engineering R*, vol. 44, no. 2-3, pp. 45–89, 2004.

[15] D. B. Chrisey and G. K. Hubler, Eds., *Pulsed Laser Deposition of Thin Films*, John Wiley & Sons, New York, NY, USA, 1994.

[16] M. I. Ojovan and W. E. Lee, "Self sustaining vitrification for immobilisation of radioactive and toxic waste," *Glass Technology*, vol. 44, no. 6, pp. 218–224, 2003.

[17] C. C. Koch, "Amorphization of single composition powders by mechanical milling," *Scripta Materialia*, vol. 34, no. 1, pp. 21–27, 1996.

[18] R. W. Jones, *Fundamental Principles of Sol-Gel Technology*, The Institute of Metals, London, UK, 1989.

[19] N. T. Andrianov, "Sol-gel method in oxide material technology," *Glass and Ceramics*, vol. 60, no. 9-10, pp. 320–325, 2003.

[20] W. J. Weber, "Models and mechanisms of irradiation-induced amorphization in ceramics," *Nuclear Instruments and Methods in Physics Research B*, vol. 166-167, pp. 98–106, 2000.

[21] K. Trachenko, "Understanding resistance to amorphization by radiation damage," *Journal of Physics Condensed Matter*, vol. 16, no. 49, pp. R1491–R1515, 2004.

[22] O. Mishima, L. D. Calvert, and E. Whalley, "'Melting ice' I at 77 K and 10 kbar: a new method of making amorphous solids," *Nature*, vol. 310, no. 5976, pp. 393–395, 1984.

[23] G. N. Greaves, F. Meneau, A. Sapelkin, et al., "The rheology of collapsing zeolites amorphized by temperature and pressure," *Nature Materials*, vol. 2, no. 9, pp. 622–629, 2003.

[24] Glass, Encyclopaedia Britannica, November 2007, http://www.britannica.com.

[25] K. L. Ngai and S. Capaccioli, "The challenging problem of glass transition," *Journal of the American Ceramic Society*, vol. 91, no. 3, pp. 709–714, 2008.

[26] J. C. Dyre, "Colloquium: the glass transition and elastic models of glass-forming liquids," *Reviews of Modern Physics*, vol. 78, no. 3, pp. 953–972, 2006.

[27] H. Tanaka, "Two-order-parameter model of the liquid-glass transition—I: relation between glass transition and crystallization," *Journal of Non-Crystalline Solids*, vol. 351, no. 43–45, pp. 3371–3384, 2005.

[28] C. M. Roland and R. Casalini, "Density scaling of the dynamics of vitrifying liquids and its relationship to the dynamic crossover," *Journal of Non-Crystalline Solids*, vol. 351, no. 33–36, pp. 2581–2587, 2005.

[29] C. A. Angel, K. L. Ngai, G. B. McKenna, P. F. McMillan, and S. W. Martin, "Relaxation in glass forming liquids and amorphous solids," *Journal of Applied Physics*, vol. 88, no. 6, pp. 3113–3157, 2000.

[30] W. Gotze and L. Sjogren, "Relaxation processes in supercooled liquids," *Reports on Progress in Physics*, vol. 55, no. 3, pp. 241–376, 1992.

[31] J. Zarzycki, *Glasses and the Vitreous State*, Cambridge University Press, New York, NY, USA, 1982.

[32] M. Kodama and S. Kojima, "Anharmonicity and fragility in lithium borate glasses," *Journal of Thermal Analysis and Calorimetry*, vol. 69, no. 3, pp. 961–970, 2002.

[33] I. Gutzow and B. Petroff, "The glass transition in terms of Landau's phenomenological approach," *Journal of Non-Crystalline Solids*, vol. 345-346, pp. 528–536, 2004.

[34] L. D. Landau and E. M. Lifshitz, *Statistical Physics. Part 1*, Butterworth-Heinemann, Oxford, UK, 1984.

[35] J. M. Stevels, "Repeatability number, Deborah number and critical cooling rates as characteristic parameters of the vitreous state," in *Amorphous Materials*, R. W. Douglas and B. Ellis, Eds., pp. 133–140, John Wiley & Sons, London, UK, 1972.

[36] K. L. Ngai, "Do theories of glass transition that address only the α-relaxation need a new paradigm?" *Journal of Non-Crystalline Solids*, vol. 351, no. 33–36, pp. 2635–2642, 2005.

[37] M. Goldstein, "Viscous liquids and the glass transition: a potential energy barrier picture," *The Journal of Chemical Physics*, vol. 51, no. 9, pp. 3728–3739, 1969.

[38] C. A. Angell, "Formation of glasses from liquids and biopolymers," *Science*, vol. 267, no. 5206, pp. 1924–1935, 1995.

[39] R. Richert, "Heterogeneous dynamics in liquids: fluctuations in space and time," *Journal of Physics Condensed Matter*, vol. 14, no. 23, pp. R703–R738, 2002.

[40] P. Duvall, J. Keesling, and A. Vince, "The Hausdorff dimension of the boundary of a self-similar tile," *Journal of the London Mathematical Society*, vol. 61, no. 3, pp. 649–760, 2000.

[41] B. B. Mandelbrot, *Fractals: Form, Chance and Dimension*, Freeman, San Francisco, Calif, USA, 1977.

[42] R. H. Doremus, "Melt viscosities of silicate glasses," *American Ceramic Society Bulletin*, vol. 82, no. 3, pp. 59–63, 2003.

[43] R. H. Doremus, "Viscosity of silica," *Journal of Applied Physics*, vol. 92, no. 12, pp. 7619–7629, 2002.

[44] Y. I. Frenkel, *Kinetic Theory of Liquids*, Oxford University Press, Oxford, UK, 1946.

[45] I. Avramov, "Viscosity in disordered media," *Journal of Non-Crystalline Solids*, vol. 351, no. 40–42, pp. 3163–3173, 2005.

[46] R. H. Doremus, *Glass Science*, John Wiley & Sons, New York, NY, USA, 1973.

[47] M. I. Ojovan, K. P. Travis, and R. J. Hand, "Thermodynamic parameters of bonds in glassy materials from viscosity-temperature relationships," *Journal of Physics: Condensed Matter*, vol. 19, Article ID 415107, 12 pages, 2007.

[48] P. Gibbs, "Is glass a liquid or a solid?" *Glass Worldwide*, vol. 11, pp. 14–18, 2007.

[49] W. D. Callister Jr., *Fundamentals of Material Science and Engineering*, John Wiley & Sons, New York, NY, USA, 2001.

[50] B. A. Shakhmatkin, N. M. Vedishcheva, and A. C. Wright, "Can thermodynamics relate the properties of melts and glasses to their structure?" *Journal of Non-Crystalline Solids*, vol. 293–295, no. 1, pp. 220–226, 2001.

[51] SciGlass 6.5 Database and Information System, November 2007, http://www.sciglass.info.

[52] D. Martlew, "Viscosity of molten glasses," in *Properties of Glass-Forming Melts*, D. Pye, I. Joseph, and A. Montenero, Eds., p. 485, Taylor & Francis, Boca Raton, Fla, USA, 2005.

[53] A. Fluegel, "Glass viscosity calculation based on a global statistical modelling approach," *Glass Technology*, vol. 48, no. 1, pp. 13–30, 2007.

[54] W. Lutze, "Silicate glasses," in *Radioactive Waste Forms for the Future*, W. Lutze and R. Ewing, Eds., pp. 1–160, Elsevier, Amsterdam, The Netherlands, 1988.

[55] C. A. Angell, "Perspective on the glass transition," *Journal of Physics and Chemistry of Solids*, vol. 49, no. 8, pp. 863–871, 1988.

[56] L.-M. Martinez and C. A. Angell, "A thermodynamic connection to the fragility of glass-forming liquids," *Nature*, vol. 410, no. 6829, pp. 663–667, 2001.

[57] J. E. Stanworth, *Physical Properties of Glass*, Oxford University Press, Oxford, UK, 1950.

[58] M. B. Volf, *Mathematical Approach to Glass*, Elsevier, Amsterdam, The Netherlands, 1988.

[59] R. W. Douglas, "The flow of glass," *Journal of the Society of Glass Technology*, vol. 33, pp. 138–162, 1949.

[60] D. Turnbull and M. H. Cohen, "Free-volume model of the amorphous phase: glass transition," *The Journal of Chemical Physics*, vol. 34, no. 1, pp. 120–125, 1961.

[61] G. Adam and J. H. Gibbs, "On the temperature dependence of cooperative relaxation properties in glass-forming liquids," *The Journal of Chemical Physics*, vol. 43, no. 1, pp. 139–146, 1965.

[62] I. Avramov, "Pressure dependence of viscosity of glassforming melts," *Journal of Non-Crystalline Solids*, vol. 262, no. 1, pp. 258–263, 2000.

[63] M. I. Ojovan, "Viscosity of oxide melts in the doremus model," *JETP Letters*, vol. 79, no. 2, pp. 85–87, 2004.

[64] M. I. Ojovan and W. E. Lee, "Viscosity of network liquids within Doremus approach," *Journal of Applied Physics*, vol. 95, no. 7, pp. 3803–3810, 2004.

[65] J. F. Stebbins, "NMR evidence for five-coordinated silicon in a silicate glass at atmospheric pressure," *Nature*, vol. 351, no. 6328, pp. 638–639, 1991.

[66] R. Zallen, *The Physics of Amorphous Solids*, John Wiley & Sons, New York, NY, USA, 1983.

[67] J. M. Ziman, *Models of Disorder*, Cambridge University Press, Cambridge, UK, 1979.

[68] P. G. Debenedetti, *Metastable Liquids*, Princeton University Press, Princeton, NJ, USA, 1997.

[69] A. V. Evteev, A. T. Kosilov, and E. V. Levchenko, "Atomic mechanisms of pure iron vitrification," *Journal of Experimental and Theoretical Physics*, vol. 99, no. 3, pp. 522–529, 2004.

[70] L. W. Hobbs, "Network topology in aperiodic networks," *Journal of Non-Crystalline Solids*, vol. 192-193, pp. 79–91, 1995.

[71] N. N. Medvedev, A. Geiger, and W. Brostow, "Distinguishing liquids from amorphous solids: percolation analysis on the Voronoi network," *The Journal of Chemical Physics*, vol. 93, no. 11, pp. 8337–8342, 1990.

[72] K. Binder, "Computer simulations of undercooled fluids and the glass transition," *Journal of Non-Crystalline Solids*, vol. 274, no. 1, pp. 332–341, 2000.

[73] A. S. Kolokol and A. L. Shimkevich, "Topological structure of liquid metals," *Atomic Energy*, vol. 98, no. 3, pp. 187–190, 2005.

[74] M. H. Cohen and D. Turnbull, "Molecular transport in liquids and glasses," *The Journal of Chemical Physics*, vol. 31, no. 5, pp. 1164–1169, 1959.

[75] G. S. Grest and M. H. Cohen, "Liquids, glasses, and the glass transition: a free-volume approach," *Advances in Chemical Physics*, vol. 48, pp. 455–525, 1981.

[76] E. Williams and C. A. Angell, "Pressure dependence of the glass transition temperature in ionic liquids and solutions. Evidence against free volume theories," *The Journal of Physical Chemistry*, vol. 81, no. 3, pp. 232–237, 1977.

[77] E. Leutheusser, "Dynamical model of the liquid-glass transition," *Physical Review A*, vol. 29, no. 5, pp. 2765–2773, 1984.

[78] U. Bengtzelius, W. Gotze, and A. Sjolander, "Dynamics of supercooled liquids and the glass transition," *Journal of Physics C*, vol. 17, no. 33, pp. 5915–5934, 1984.

[79] H. Tanaka, "Two-order-parameter model of the liquid-glass transition—II: structural relaxation and dynamic heterogeneity," *Journal of Non-Crystalline Solids*, vol. 351, no. 43–45, pp. 3385–3395, 2005.

[80] H. Tanaka, "Two-order-parameter model of the liquid-glass transition—III: universal patterns of relaxations in glass-forming liquids," *Journal of Non-Crystalline Solids*, vol. 351, no. 43–45, pp. 3396–3413, 2005.

[81] A. V. Evteev, A. T. Kosilov, E. V. Levchenko, and O. B. Logachev, "Kinetics of isothermal nucleation in a supercooled iron melt," *Physics of the Solid State*, vol. 48, no. 5, pp. 815–820, 2006.

[82] H. Tanaka, "Possible resolution of the Kauzmann paradox in supercooled liquids," *Physical Review E*, vol. 68, no. 1, Article ID 011505, 8 pages, 2003.

[83] F. C. Frank, "Melting as a disorder phenomenon," *Proceedings of the Royal Society of London. Series A*, vol. 215, no. 1120, pp. 43–46, 1952.

[84] P. J. Steinhardt, D. R. Nelson, and M. Ronchetti, "Bond-orientational order in liquids and glasses," *Physical Review B*, vol. 28, no. 2, pp. 784–805, 1983.

[85] S. A. Kivelson, X. Zhao, D. Kivelson, T. M. Fischer, and C. M. Knobler, "Frustration-limited clusters in liquids," *The Journal of Chemical Physics*, vol. 101, no. 3, pp. 2391–2397, 1994.

[86] D. Kivelson, S. A. Kivelson, X. Zhao, Z. Nussinov, and G. Tarjus, "A thermodynamic theory of supercooled liquids," *Physica A*, vol. 219, no. 1-2, pp. 27–38, 1995.

[87] E. Donth, *The Glass Transition*, Springer, New York, NY, USA, 2001.

[88] A. Hunt, "Some comments on the dynamics of super-cooled liquids near the glass transition," *Journal of Non-Crystalline Solids*, vol. 195, no. 3, pp. 293–303, 1996.

[89] A. Hunt, "The pressure dependence of the glass transition temperature in some ionic liquids," *Journal of Non-Crystalline Solids*, vol. 176, no. 2-3, pp. 288–293, 1994.

[90] A. Hunt, "Finite-size effects on the glass transition temperature," *Solid State Communications*, vol. 90, no. 8, pp. 527–532, 1994.

[91] A. Hunt, "A purely kinetic justification for application of Ehrenfest theorems to the glass transition," *Solid State Communications*, vol. 84, no. 3, pp. 263–266, 1992.

[92] C. A. Angell and K. J. Rao, "Configurational excitations in condensed matter, and the "bond lattice" model for the liquid-glass transition," *The Journal of Chemical Physics*, vol. 57, no. 1, pp. 470–481, 1972.

[93] Y. Kraftmakher, "Equilibrium vacancies and thermophysical properties of metals," *Physics Report*, vol. 299, no. 2-3, pp. 79–188, 1998.

[94] C. A. Angell and J. Wong, "Structure and glass transition thermodynamics of liquid zinc chloride from far-infrared, raman, and probe ion electronic and vibrational spectra," *The Journal of Chemical Physics*, vol. 53, no. 5, pp. 2053–2066, 1970.

[95] M. B. Isichenko, "Percolation, statistical topography, and transport in random media," *Reviews of Modern Physics*, vol. 64, no. 4, pp. 961–1043, 1992.

[96] M. Sahimi, *Applications of Percolation Theory*, Taylor & Francis, London, UK, 1994.

[97] H. Scher and R. Zallen, "Critical density in percolation processes," *The Journal of Chemical Physics*, vol. 53, no. 9, pp. 3759–3761, 1970.

[98] A. Koike and M. Tomozawa, "Towards the origin of the memory effect in oxide glasses," *Journal of Non-Crystalline Solids*, vol. 354, no. 28, pp. 3246–3253, 2008.

[99] B. I. Shklovskioe and A. L. Éfros, *Electronic Properties of Doped Semiconductors*, Springer, New York, NY, USA, 1984.

[100] A. Z. Patashinskioe and V. L. Pokrovskioe, *Fluctuation Theory of Phase Transitions*, Pergamon, Oxford, UK, 1979.

[101] M. I. Ozhovan, "Dynamic uniform fractals in emulsions," *Journal of Experimental and Theoretical Physics*, vol. 77, no. 6, pp. 939–943, 1993.

[102] V. V. Brazhkin and A. G. Lyapin, "A universal increase in the viscosity of metal melts in the range of megabar pressures: a glassy state of the earth's inner core," *Uspekhi Fizicheskikh Nauk*, vol. 170, no. 5, pp. 535–551, 2000.

[103] I. Avramov, "Pressure dependence of viscosity, or is the earth's mantle a glass?" *Journal of Physics Condensed Matter*, vol. 20, no. 24, Article ID 244106, 4 pages, 2008.